Forest vegetation change and surface hydrology following 47 years of managed wildfire

Journal:	*Ecosystems*
Manuscript ID	ECO-19-0209
Types:	Original Article
Date Submitted by the Author:	21-Jun-2019
Complete List of Authors:	Stevens, Jens; US Geological Survey Southwest Region, New Mexico Landscapes Field Station; University of California Berkeley, Boisrame, Gabrielle; University of California Berkeley, Civil and Environmental Engineering Rakhmatulina, Ekaterina; University of California Berkeley, Civil and Environmental Engineering Thompson, Sally; University of California Berkeley, Civil and Environmental Engineering Collins, Brandon; USDA Forest Service, Pacific Southwest Research Station; University of California Berkeley, Center for Fire Research and Outreach Stephens, Scott; University of California, Berkeley, ESPM
Key Words:	ecohydrology, fire, soil moisture, vegetation change, forests, Sierra Nevada

Running Head

Vegetation and soil moisture under active fire regime

Title

Forest vegetation change and surface hydrology following 47 years of managed wildfire

Authors

Jens T. Stevens [1*, 2], Gabrielle Boisramé[2, 3], Ekaterina Rakhmatulina[3], Sally Thompson[3,4], Brandon Collins[2], Scott Stephens[2]

Author Affiliations and Addresses

[1]U.S. Geological Survey, New Mexico Landscapes Field Station, Santa Fe NM 87508

[2]University of California Berkeley, Department of Environmental Science, Policy and Management, Berkeley CA, 94720

[3]University of California Berkeley, Department of Civil and Environmental Engineering, Berkeley CA, 94720

[4]University of Western Australia, Department of Civil, Environmental and Mining Engineering, Crawley, Western Australia, 6009

*Corresponding Author: E-mail: jtstevens@usgs.gov, Telephone: 505-954-2252.

Target journal: Ecosystems (req's: 250 word abstract, 8000 word (35 pg double spaced) max)

Abstract

Managed wildfire is an increasingly relevant management option to restore variability in vegetation structure within fire-suppressed montane forests in western North America. Managed wildfire often reduces tree cover and density, with implications for land surface – atmosphere exchange, snowpack, and evapotranspiration, potentially leading to increases in soil moisture availability, water storage in soils and groundwater, and streamflow. Yet the potential hydrologic impacts of managed wildfire in montane watersheds remain under-studied, despite the significance of such watersheds for regional water supply. Here we characterize the response of vegetation and soil moisture to 47 years (1971-2018) of managed wildfire in Sugarloaf Creek Basin (SCB) in Sequoia-Kings Canyon National Park in the Sierra Nevada, California, USA, using remote-sensing of vegetation, repeat plot-measurements, and a combination of continuous in-situ and episodic spatially-distributed soil moisture measurements. We find that, by comparison to a wetter nearby watershed experiencing similar fire management, the managed wildfire regime at SCB caused relatively little change in dominant vegetation, and relatively little response of soil moisture. Fire occurrence was limited to drier mixed-conifer sites; fire-caused overstory tree mortality patches were generally < 10 ha, and fires had little effect on removing mid- and lower strata trees. Few dense meadow areas were created by fire, with most forest conversion leading to sparse meadow and shrub areas, which had similar soil moisture profiles to nearby mixed-conifer vegetation. Future fires in SCB could be managed to encourage greater tree mortality, although the potential hydrologic benefits of the program in this basin may be limited.

Introduction

Many forests in California's Sierra Nevada, like other dry mixed-conifer forests of the western United States, have experienced fire exclusion since the end of the 1800s, and were managed under an active policy of fire suppression throughout the Twentieth Century (McKelvey et al. 1996). The consequences of fire exclusion for the vegetation of the Sierra Nevada are well known and include increases in forested area, increases in forest stem density and uniformity of stands, and reductions in landscape heterogeneity (Collins et al. 2011, Safford and Stevens 2017). By creating large connected patches of dense fuels, fire exclusion and suppression have also set the stage for a dramatic escalation in the frequency and extent of severe fires (Westerling and Swetnam 2003, Stephens et al. 2013, North et al. 2015, Stephens et al. 2016) – for example, five of the ten largest and most destructive fires in California (as of fall 2018), occurred after 2010 (CalFire 2018a, 2018b). The scale of fire-caused tree mortality in these and many other contemporary fires is well outside the historical range of variability in Sierra Nevada forests (Collins et al. 2011, Safford and Stevens 2017). Recent large-scale stand-replacing fire effects, combined with the densification and homogenization brought about by widespread fire suppression, have negatively impacted biodiversity, water resources and forest resilience (Grant et al. 2013, Ponisio et al. 2016). Such negative impacts have motivated the adoption of a broad suite of forest management practices ranging from mechanical forest thinning to prescribed fire (Stephens et al. 2016) to restore a forest structure resilient to future fires.

An additional forest restoration strategy, managed wildfire, is drawing increased attention (North et al. 2012, Boisramé et al. 2017). Managed wildfire involves allowing naturally ignited wildfires to burn unimpeded unless specific predefined criteria (for example relating to hazard or air quality) are met and trigger intervention. In the Sierra Nevada, two wilderness areas, the

Illilouette Creek and Sugarloaf Creek Basins - in Yosemite and Sequoia-Kings Canyon National Parks, respectively - have used managed wildfire for nearly 50 years. The resulting wildfire regime in these basins has near-historical fire frequencies (Collins et al. 2007). In addition, the emergence of non-overlapping fire extents in these basins suggests self-limiting behavior as the fuel distribution becomes more fragmented in space (Collins et al. 2007, Collins et al. 2009, Collins et al. 2011, Parks et al. 2015, Collins et al. 2016). While these outcomes suggest that managed wildfire has had a positive effect in restoring historical fire regimes and mitigating fire hazard, its co-benefits on other ecosystem services, prominently the regulation of water, given the importance of these forests for water supply in California and the western US more generally, remain less certain.

In the Illilouette Creek Basin (ICB), the imposition of managed wildfire led to large (24%) decreases in forested area and the replacement of forests with new areas of shrubland, grassland and dense meadows/wetlands (Boisramé et al. 2017b). In the ICB today, vegetation type is closely associated with soil moisture regimes (Boisramé et al. 2018), allowing changes in hydrological condition associated with the forest cover conversion to be estimated. The contemporary vegetation cover suggests that water storage and plant available water resources increased in the ICB in response to managed wildfire (Boisramé et al. 2018). This finding is consistent with comparisons to similar but fire-suppressed Sierra Nevada river basins (Boisramé et al. 2017), and with mechanistic ecohydrological modeling of ICB (Boisrame et al. 2019 *in press*), which suggest that soil moisture and streamflow have increased, and plant water stress decreased, in response to the changed fire regime.

These results suggest of a promising co-benefit for water resources associated with restoration of a near-natural fire regime in the ICB. However, it is unclear how the effects of managed wildfire will play out in other Sierra Nevada forests. ICB is a relatively wet, mid-elevation watershed containing productive forests. Different climates, soils and vegetation types found at other elevations and locations in the Sierra Nevada could exhibit different responses to a changed fire regime. Sugarloaf Creek Basin (SCB) in Sequoia-Kings Canyon National Park offers a chance to explore the impact of managed wildfire in a less productive, drier and slightly higher-elevation watershed than ICB. In this study, we draw on historical and contemporary aerial photography and vegetation classifications, historical and contemporary forest plot surveys, and contemporary soil moisture and meteorological observations within SCB to address four questions:

(1) Has vegetation cover changed in the SCB from 1973-present at the landscape scale, and if so, how are these changes associated with fire?
(2) How has forest composition and structure at the survey plot scale changed from 1970-present, and how are these changes associated with fire?
(3) Are different vegetation cover types in the SCB associated with differences in soil moisture, and what does this imply about hydrologic response to wildfire in the SCB?, and finally
(4) How do changes in landscape vegetation cover (1) and soil moisture (3) compare with those previously described in the Illilouette Creek Basin?

Methods

Study site and climate

The Sugarloaf Creek Basin (SCB) covers 125 km^2, spanning elevation ranges of 2000 – 3200 m in Sequoia and Kings Canyon National Parks. Average daily temperatures range from minimum of -10^o C to 31^o C, with the annual average being 14.5^o C (Global Historical Climate Network, station USR0000CSUG). Vegetation in this region varies with elevation, topography, and soil type (Stephenson 1998, Caprio and Graber 2000). The dominant tree species found in SCB are Jeffrey pine (*Pinus jeffreyi*), lodgepole pine (*Pinus contorta*), white fir (*Abies concolor*), and red fir (*Abies magnifica*), which occur interspersed with meadows and shrublands. Based on tree ring reconstructions, fire was common in this area prior to 1900, with a mean fire interval of 9 years for the period 1700-1900 (Collins and Stephens 2007). Fire suppression appears to have manifested in SCB shortly after 1900, resulting in an anomalously long fire-free period lasting until the early 1970's (Collins and Stephens 2007), with no evidence of logging in this period.

In 1968 the National Park Service changed its fire policy and began to use prescribed fires and managed lightning fires to meet ecological goals; previously all fires had been suppressed (van Wagtendonk 2007). Yosemite National Park (including the 150 km^2 ICB) is the only other place in the Sierra Nevada that has had a policy of allowing lightning-ignited wildfires to burn for as long as Kings Canyon National Park (van Wagtendonk 2007). The first notable fire in SCB under the fire use policy was the Ball Dome Fire in 1971, which burned nearly 100 ha. Since then, nine other fires over 40 ha in size burned partially or completely in SCB, the largest of which was over 4000 ha (Appendix A, Table A1). For comparison, ICB had 27 fires >40 ha between 1970 and 2016 (Collins et al. 2016).

We obtained fire perimeters for all SCB fires between 1952 and 2016 from a statewide database maintained by the California Department of Forestry and Fire Protection (FRAP 2017).

These perimeters were corroborated with those maintained by park staff (personal communication, A. Caprio, Sequoia and Kings Canyon National Park). Because our historical imagery dates to 1973 (see below), we removed four small (<100 ha) fires that burned between 1952-1972 from our imagery analyses (Figure 1; Table A1). Our historical forestry plots date to 1970 (see below), but none were located within the perimeters of these four fires (Figure 1). We also removed two fires, from 2004 and 2006, that were both $<0.05 km^2$ and located on the margins of the watershed (not shown in Figure 1). Of the 12 fires included for analysis, the mean fire size was 825 ha.

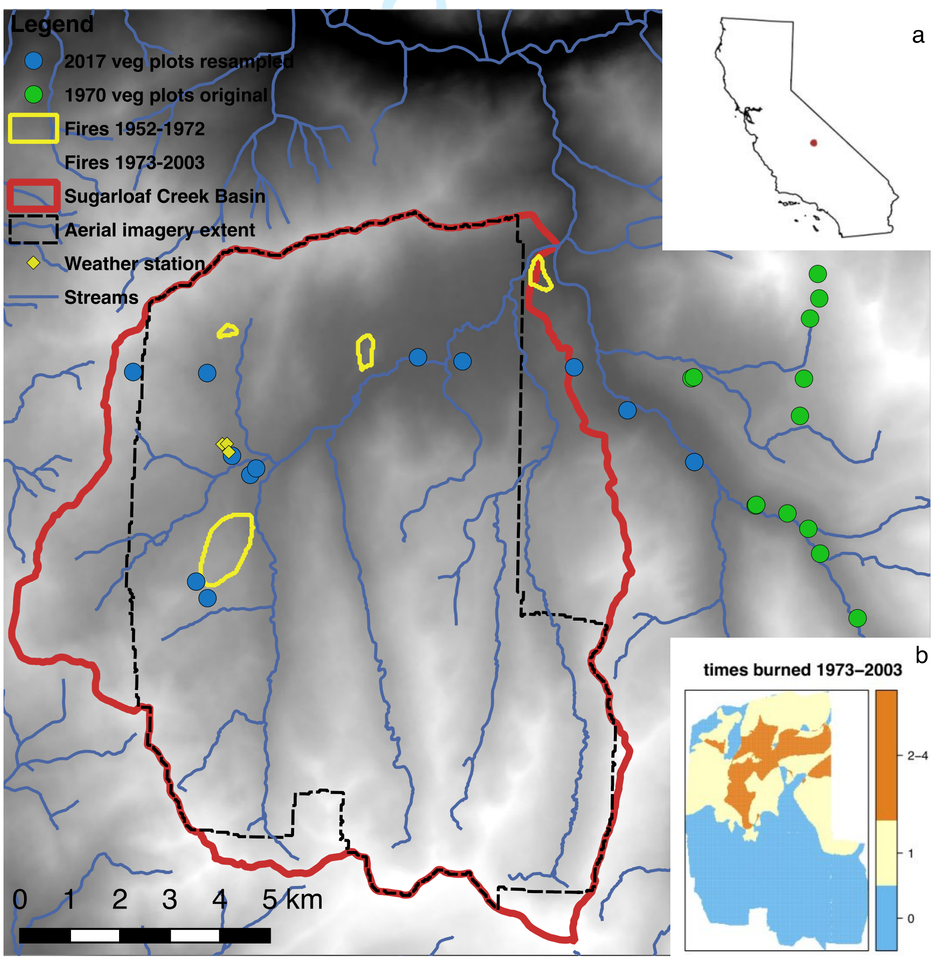

***Figure 1**: Sugarloaf Creek Basin (SCB) shown in red (and in panel a). Base layer DEM ranges from 1480 m (black) to 3375 m (white; Data source: ASTER GDEM, a product of METI and NASA). Overlapping fire perimeters since 1973 shown in transparent red. Inset (b) shows composite of overlapping fires from 1973-2003, with colors indicating number of times burned, over the extent represented by the 1973 aerial imagery. Points in main figure indicate main vegetation (forestry) plots, a subset of which (blue) were re-sampled in 2017.*

Differences in water balance between SCB and ICB may contribute to differences in how near-natural fire regimes have impacted these two Sierra Nevada watersheds. ICB is slightly lower in elevation (1800-3500 m, mean = 2500 m) than SCB (2000 – 3500 m, mean = 2700 m), but has similar vegetation (Collins et al. 2016). We installed temporary weather stations (Appendix B) at elevations of 2100 m in ICB and 2400 m in SCB, which showed similar temperatures (data not shown), but greater precipitation (Table 1) at ICB than SCB for the duration of our field data collection (2016-2018). Annual precipitation in SCB has not been measured in the long term; with the nearest precipitation gage (Cedar Grove) operating only in summer months. A sense of the long-term water balance of the basin, however, can be gained from streamflow measured in the South Fork Kings River downstream of the confluence of Sugarloaf Creek with this river. Two gages were operational on the South Fork Kings River through the late 1950s, and two gages on the Merced River are located downstream of where flow from ICB enters the Merced River (although they measure flow draining slightly smaller areas than the Kings River gages; Table A2). Specific discharge (total streamflow divided by watershed area) measured at or downstream of ICB is greater (0.65-0.9 m/yr) than that measured downstream of SCB (0.48-0.55 m/yr; Table A2), suggesting that the region containing SCB is more water-limited.

Vegetation cover change

To compute the change in vegetation cover in SCB since the first large fire in 1973 (Question 1), we classified aerial photographs into granite (exposed rock), water, sparse meadows, dense meadows, conifer forest, and shrublands, following the methods used by Boisramé et al. (2017b). We obtained the earliest set of aerial photographs available for the region from Sequoia Kings Canyon National Park. These black and white photos were dated to 1973, prior to the first fires occurring in SCB, scanned at 600 dpi, and covered 10,120 ha (81%)

of the 12,500-ha watershed (Figure 1). Contemporary cover was represented by color imagery from the 2014 National Agriculture Imagery Program, and clipped to the same extent as the 1973 imagery. The 1973 images were orthorectified using ERDAS IMAGINE software, using approximately 15-20 control points per image. We used the eCognition object-oriented software package (produced by Trimble, www.ecognition.com) to classify the images into objects of similar color band values, texture and shape (Blaschke et al. 2014). Our supervised classification approach produced objects in the following categories: mixed-conifer forest, shrub, sparse meadow, dense meadow, rock and open water. Following classification, the 1973 images (representing approximately 16.7 km^2 each) were mosaicked together in ArcGIS, as were the 2014 images (representing approximately 39 km^2 each).

During post-processing, the vector-object layers produced by eCognition were converted to raster layers in ArcGIS, with a 40 m pixel resolution, ensuring alignment of the 1973 and 2014 rasters to enable a change detection analysis. Because the rasterization process created single isolated pixels of a given class derived from polygon slivers, we smoothed the resulting raster surface using the *adjacent* function in the R library *raster* (Hijmans and van Etten 2014). We removed isolated pixels surrounded by other vegetation in the four cardinal directions, changing the pixel in question to the most common vegetation type surrounding it.

We used the spatial layers from 1973 and 2014 to determine the direction and proportionality of vegetation change in the intervening 41 years. We then analyzed the relationship between these changes and the number of times each pixel had burned. We overlaid the fire perimeter polygons on the two vegetation raster layers to extract a “times burned” attribute for each pixel. Due to subsequent chi-squared tests not converging for analyses of pixels burned 3 times (218 ha) and 4 times (15 ha), we combined these categories into a single “2-4 times burned" category, in addition to analyses conducted for once-burned pixels, unburned pixels, and the entire mapped area. We excluded pixels classified as granite or water from this analysis, leaving four vegetation classes which could transition from one to another: shrubs, sparse meadow, mixed conifer and dense meadow. We calculated the number of pixels that underwent each possible transition among those four categories (including pixels that remained the same). Our null expectation of vegetation change was that a transition between two vegetation types was equally likely in each direction, with this transition probability estimated by summing the number of pixels in each direction of change between a given pair of vegetation types, and dividing by two. We then compared the distribution of pixels in each of the resulting sixteen potential vegetation transition classes against an expected distribution (holding the number of unchanged pixels constant) using a chi-squared test. We determined the residual proportion of expected change, compared to the null expectation, as a percentage (increase or decrease) from the null expectation for a given transition class.

As a basis for comparing the post-fire vegetation landscapes at SCB and ICB (question 4), we assessed landscape metrics in SCB to describe the heterogeneity of the landscape and spatial distribution of individual vegetation classes, in both 1973 and 2014, using FRAGSTATS (McGarigal et al. 2012), and compared these to values calculated for ICB (Boisramé et al. 2017b). At the landscape level, these metrics included the evenness index and the aggregation index, and at the vegetation class level they included mean, standard deviation, and maximum of patch area, and mean patch fractal dimension.

Forestry plots

In areas that did not convert to alternative vegetation types, we explored the question of how forest structure has changed over time in response to fire (Question 2) by resampling a historic forest plot dataset. Forest surveys were conducted in Sugarloaf Creek Basin in July 1970 by Hammond, Jensen & Wallen Mapping and Forestry Services, Oakland CA. Surveyors measured 25 plots (Figure 1), which consisted of five 0.2 ac (0.08 ha) subplots each. Each subplot was surveyed for conifer trees (stems > 7.6 cm DBH), saplings (stems 0.6 m tall up to 7.6 cm DBH, where DBH was not recorded), and seedlings (stems <0.6 m tall). The surveyors estimated representative tree heights and woody (shrub) ground cover within the plots. All shrubs and trees were identified to species level. Subplots were arranged along linear transects with generally 40 m spacing between them, from an anchor point and a given transect azimuth that was described in the field notes. We re-surveyed 12 of these plots in 2017 (Figure 1) following the same methods, leading to a total of 58 subplots sampled in both 1970 and 2017, which constituted our sample size for analysis.

For each subplot, we used the collection of fire perimeters from Sugarloaf Creek Basin to identify the number of times each subplot had burned since fire was reintroduced in 1973 (0, 1, or 2-4). We calculated density of all trees (>7.6 cm DBH), medium trees (>15.2 cm DBH), large trees (>61 cm DBH), and very large trees (>100 cm DBH), and calculated basal area of each of these size classes by species as well. For each size class we compared the change in density and basal area over time, using linear mixed-effects models that assigned a random intercept to subplot ID, accounting for repeated sampling of the same plots over time by allowing a given plot to have higher or lower overall values of the response variables, using the R package *lme4* (Bates et al. 2013). We evaluated the significance of these trends using the Kenward-Rodgers approximation to estimate degrees of freedom in the mixed-effects models, via the R package *pbkrtest* (Halekoh and Højsgaard 2014).

Soil moisture

Spatially-distributed soil moisture measurements

To assess the drivers of spatial variability in shallow soil moisture (Question 3), we sampled soil moisture in the field at 40 sites in 2016, 2017, and 2018, which included three sites where we installed temporary weather stations (see below). We measured soil moisture in the top 12 cm of soil using Hydrosense 2 Time-Domain Reflectometer (TDR) probes (campbellsci.com/hs2). We measured most of these sites in both early and late summer (some sites had to be omitted during certain site visits due to safety concerns or time constraints). Twenty-nine of these sites were re-measured in June of 2018. In most sites, 25 evenly-spaced measurements of soil moisture were made within a 30m by 30m grid, with additional measurements made in heterogeneous sites in order to better capture variability. One-meter spaced measurements were made across a 30 m transect in sites with obvious strong gradients in soil moisture (e.g. wetland sites bordered by dry uplands).

At each site we categorized the vegetation of the site into one of the four classes used in our imagery analysis (n = 3 plots for shrub only, 1 plot for sparse meadow only, 2 plots for dense meadow only, 28 plots for mixed-conifer only, 2 plots split between sparse meadow and dense meadow, and 4 plots split between mixed-conifer and dense meadow). We also quantified slope, aspect, and recorded the presence of burned snags or fire-scarred trees. Sites were georeferenced using handheld Garmin GPSMAP 62st and 64st devices (horizontal accuracy 3–10 m). Latitude and longitude were assigned to each measurement point based on location within the grid or transect, and verified in ArcMap. We used these geographic positions to calculate additional topographic variables including topographic position index (TPI; a continuous variable ranging from concave to convex), upslope area (i.e. area contributing drainage to the plot), and topographic wetness index (TWI; ln[upslope area / tan[slope]]),.

We analyzed how soil moisture varied across SCB among sampling dates, vegetation types, and other environmental variables, using a random forest model implemented in the R package *RandomForest* (Liaw and Wiener 2002). Specifically, we created the model to predict continuous soil moisture using the following covariates: 2014 vegetation type, 1973 vegetation type, measurement year, day of measurement (days since December 31 of the previous year), elevation, slope, aspect, TPI, upslope area, TWI, year since fire, number of times burned since 1973, maximum fire severity (only available for fires after 1984, from the US Forest Service Pacific Southwest Region Fire Severity Mapping Program) (Miller et al. 2009), and distance from nearest stream. We cross-validated the model by selecting a subset of sites as training data and using the resulting model to predict soil moisture at the remaining sites. To compare the drivers of soil moisture at SCB and ICB (Question 4), we examined the ability of a similar soil moisture model trained on ICB data (Boisramé et al. 2018) to explain soil moisture variation observed at SCB.

We also used the random forest model to extrapolate our soil moisture measurements to unmeasured areas of the watershed, and estimate soil moisture changes due to fire changes. We modeled soil moisture on a 40m grid across the entire area of the watershed where vegetation was mapped. To estimate soil moisture levels in the absence of fire, we set times burned and fire severity to 0, time since fire to 100 years, and vegetation cover to 1973 vegetation in the random forest prediction. We then compared these modeled “unburned” conditions to soil moisture estimates that incorporated contemporary vegetation and fire histories.

Continuous soil moisture measurements

In addition to low-frequency, spatially-distributed moisture sampling described above, we addressed Question 3 by measuring in-situ, continuous soil moisture dynamics in soils at three weather stations installed in September 2016. The three weather stations are located within 250m of each other, in an area that was burned once since 1973, by the Williams fire in 2003 (Figure 1), with one weather station each in dense meadow, mixed conifer regeneration and shrubs, and mature mixed conifer vegetation types (see details and visuals in Appendix B). For simplicity, the dense meadow site is referred to as the "wetland", the shrub/conifer regeneration site as the "shrub" site, and the mixed conifer site as the "forest" site for the rest of the paper.

At these weather stations, we collected data on soil moisture, soil texture, and precipitation. Soil moisture was measured at 10-min intervals by horizontally installed Campbell Scientific 300 mm two-prong TDR probes (CS650) at 3 different depths (12, 60, and 100 cm). Soil samples were collected during the installation of the sub-surface TDR probes, and analyzed for soil texture properties at the UC Davis Analytical Laboratory (Davis, CA, USA). Precipitation was measured at 10-minute intervals by a 0.1-inch Campbell Scientific TE525 tipping bucket rain gauge (6-inch diameter orifice). The installed rain gauges are not heated, meaning that the precipitation record includes rainfall and snow-melt, but not solid-phase snow. Therefore, we augmented snowpack dynamics by recording four visual images of the stations and surrounding area per day using time-lapse cameras (Brinno TLC200), allowing us estimate snow depth at each station and derive equivalent water depth (Appendix B). In-situ data was corrected for limitations regarding gaps in snowpack data (Appendix B).

The weather station soil moisture record is substantially complete for the period September 2016-September 2018, with no more than 1.3% of data points missing for a given weather station. However, up to 32% of the precipitation time series was missing in the 2016-2018 period, due to a combination of snowmelt run-off outside of the precipitation gauge, a frozen tipping mechanism, and/or external damage to the tipping bucket and associated wiring from wildlife and extreme weather. To gap-fill missing precipitation data, we used multiple imputation via predictive mean matching (Little 1988) on precipitation observations from the neighboring stations (Appendix B). We also calculated cumulative shallow soil moisture gain between 12 and 60 cm using depth- and time-integrated soil moisture timeseries (Appendix B). Cumulative soil moisture is a useful metric to gauge how much water shallow soils have received, and to approximate precipitation amounts in unsaturated soils when the tipping bucket record is missing or not reliable. In saturated wetland sites, however, cumulative water gain cannot be calculated.

The weather station soil moisture record provides important context for interpreting the spatially-distributed soil moisture measurements. Specifically, it allows us to explore relationships between soil moisture at very shallow depths (the top 12 cm as measured in our spatially-distributed measurements) and soil moisture throughout the top 1m. Since soil moisture could behave idiosyncratically across the depth profile (Bales et al. 2011), this comparison helped determine whether the spatially-distributed measurements across the watershed are reasonable proxies for soil moisture storage and plant available water at greater soil depths. Furthermore, these stations were built and sited in a similar manner to three weather stations at ICB and provide an additional point of comparison between the two basins (Question 4).

Results

Vegetation cover change

Within the 10,120 ha of the watershed where we classified vegetation via remote sensing imagery, 1240 ha (12%) burned 2-4 times, 3173 ha (31%) burned once, and 5707 ha (57%) did not burn between 1973 and 2014 (Figure 1 inset). Approximately 3000 ha of the total area were either classified as rock or open water, a small fraction of which occurred inside burn perimeters (Figure 2). The types of vegetation transitions we observed in the watershed were generally observed across all of the three burn classes (0, 1, and 2-4 times burned; Figure 2). In particular, transitions from shrub to sparse meadow, mixed-conifer to sparse meadow, and mixed-conifer to shrub were overrepresented in the watershed (independent of fire history) compared to the null expectation, and transitions in the opposite direction were underrepresented ($X^2 = 236$, df = 15, $P < 0.001$). These trends were significant for unburned, once-burned and 2-4 times burned areas ($X^2 = 47$, 272, and 88 respectively; all df = 15, all $P < 0.001$). However, transitions towards earlier-seral vegetation types, particularly shrub to sparse meadow and mixed conifer to sparse meadow, were more strongly overrepresented in the burned areas than in the unburned areas (Figure 3, bottom row). Dense meadows did not show a consistent response to fire but in general there was limited dense meadow area to begin with and limited expansion or contraction of this vegetation type in absolute terms (Figure 3).

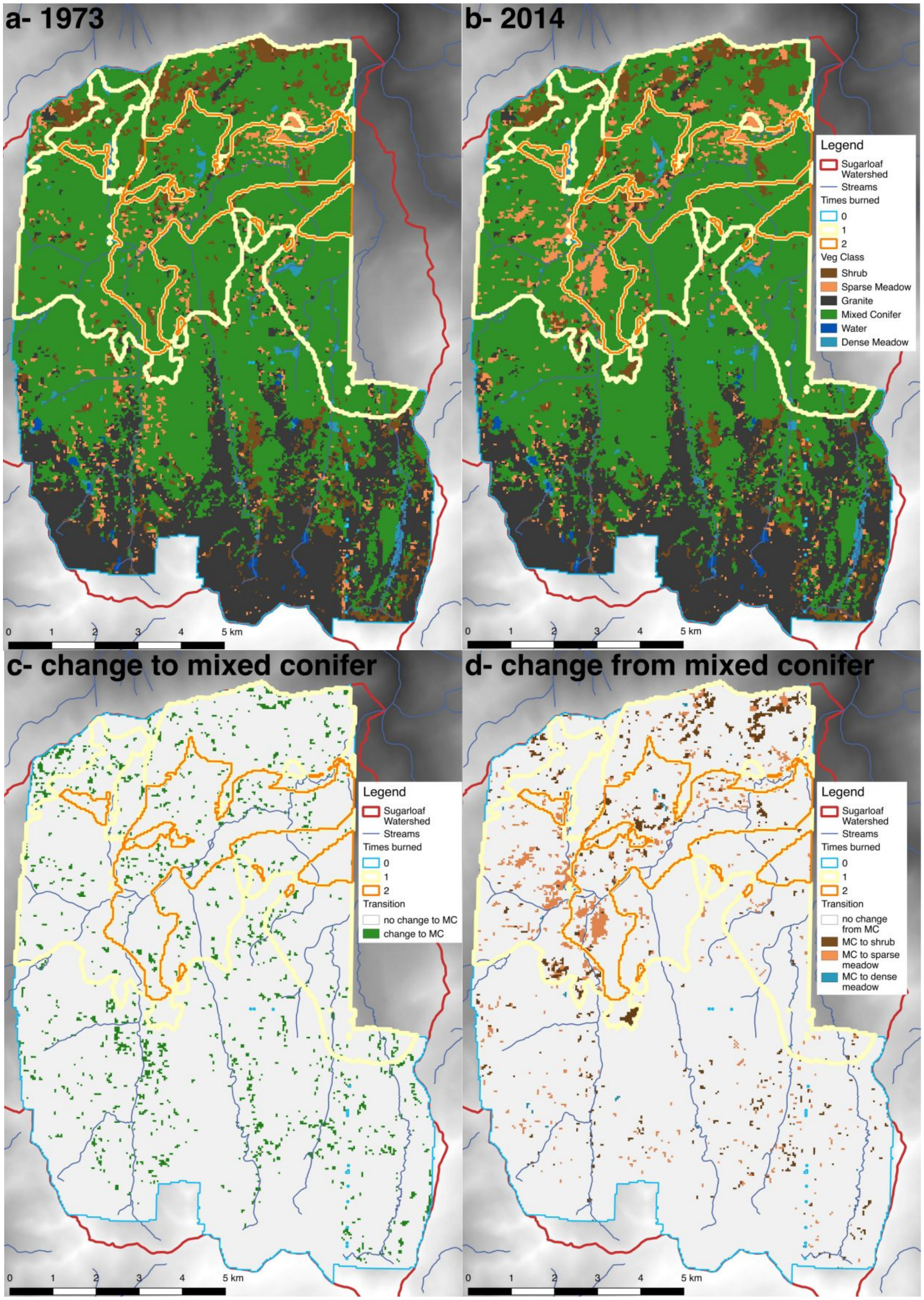

Figure 2*: Comparison of classified aerial images from 1973 (a) and 2014 (b). Perimeters of fires that burned between 1973 and 2014 are shown, aggregated by number of times burned (2 times represents combined 2-4 times burned). Four vegetation classes (shrub, sparse meadow, mixed conifer (MC), and dense meadow) are shown, along with granite and water. Transitions from non-forest to MC (c) and from MC to non-forest (d) are highlighted.*

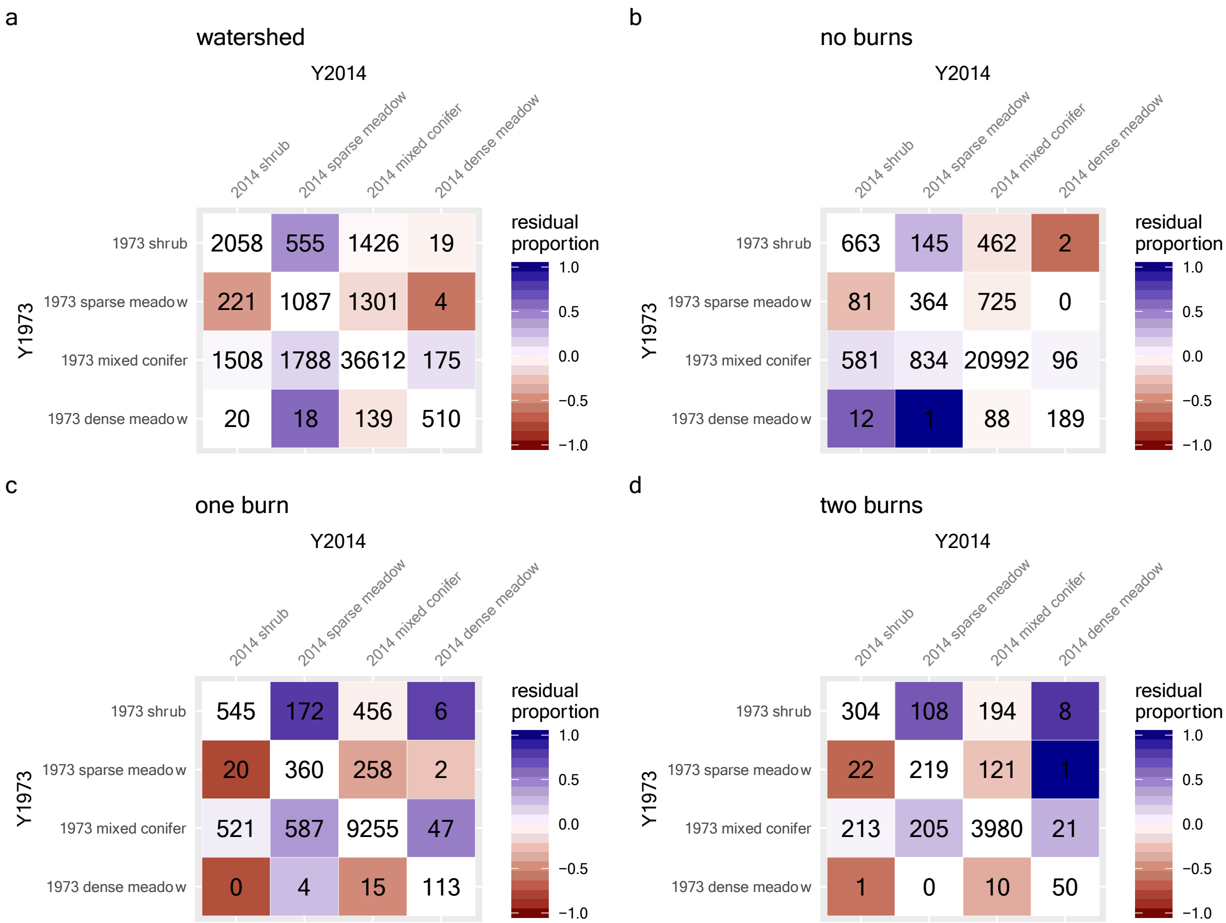

Figure 3. *Image change analysis. Colors indicated change in observed vegetation transitions relative to a null expectation of equally likely change in each direction. Color scale the proportion of the null expectation at which a given transition occurred, either more (blue) or less (red) than expected. Cell numbers indicate the number of 0.16 ha pixels in each transition category. Transitions occur from vegetation type in row (from 1973) to vegetation type in column (from 2014).*

Landscape-scale indices of heterogeneity increased slightly in 2014 compared to 1973, though the changes were much less pronounced than those that occurred in the ICB over a similar time period of repeated wildfires (Appendix C). The major differences in land cover patterns for SCB were that the mean size of conifer patches decreased from 15ha to 13ha (Figure C4a), and sparse meadows experienced small increases in both total area (7.6% to 9.0% of the vegetated area; Figure C6) and mean patch size (0.38 ha to 0.52 ha; Figure C4c).

Forest composition and structural change

Surprisingly, the number of times the forestry plots burned did not have a strong impact on changes in basal area or density in most size classes (Figure 4). Only for large trees >61 cm DBH was there a significant influence of number of times burned, where density and basal area decreased from 1970 to 2017 when burned 2 times but not 0 or 1 time (Figure 4 g, h). This effect of number of times burned was likely driven by trees in the 61-100 cm size class, because strikingly for very large trees >100 cm DBH, there was a significant decrease in density and basal area regardless of number of times burned, including in unburned plots (Figure 4 j, k). Furthermore, even in plots that had burned twice, there was an increase in total tree density. This may have been due to post-fire increases in density of the fire-intolerant *Pinus contorta*, which increased in basal area over the 47 years (Figure 4c).

The number of times a plot burned was not independent of the forest species composition: even prior to the reintroduction of large managed wildfires in 1973, plots that would eventually burn twice were located in predominantly *Pinus jeffreyi* type forest, plots that would eventually burn once were located in mixed-conifer forest with comparable proportions of *P. jeffreyi, P. contorta, Abies magnifica* and *Abies concolor,* and plots that did not burn in the 47 years were located in *Abies magnifica*-dominated forest (Figure 4c). There was also a strong difference in initial abundance of shrubs in the different forest types, with shrubs being absent in 1970 from all subplots in *Abies magnifica* forest that did not burn in the subsequent 47 years, but present in about 50% of the plots that eventually burned (Figure 5). The reintroduction of even a single wildfire was sufficient to increase shrub abundance to ~80% of subplots in 2017 (Figure 5).

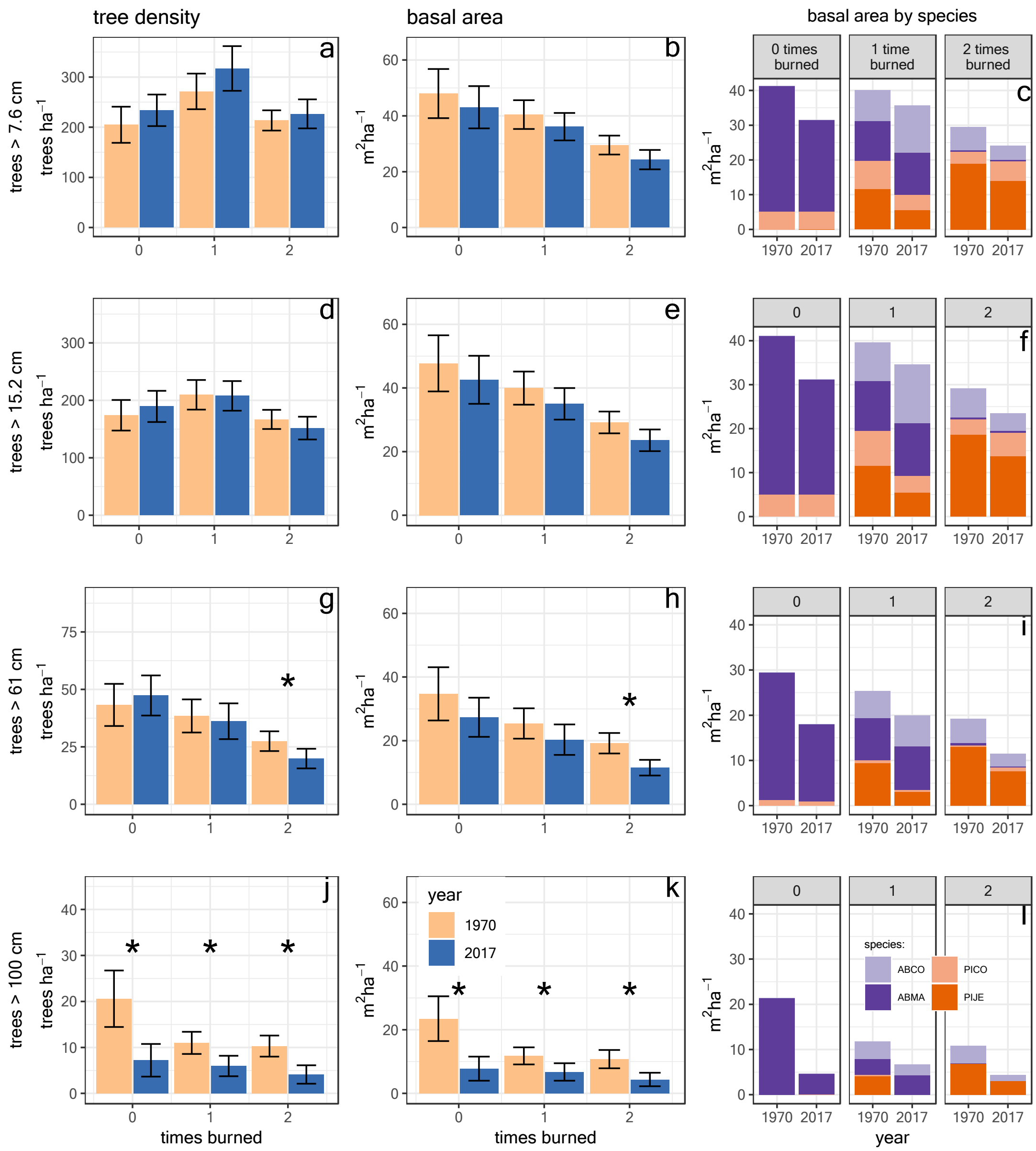

***Figure 4**: Change in forest structure based on forestry plots. Column 1 shows changes in density, column 2 shows changes in basal area, and column 3 shows changes in species composition by basal area fraction. Row 1 is for all trees >7.6 cm, row 2 is for trees > 15.2 cm, row 3 is for trees >61 cm, and row 4 is for trees >100 cm. Asterisks in columns 1 and 2 indicate significant differences in the response variable between 1970 and 2017. Note the different axis scaling in panels (g) and (j).*

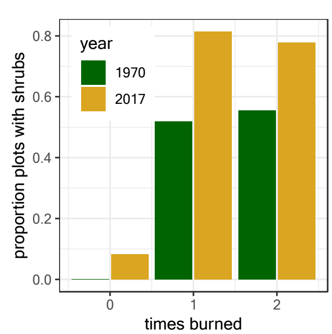

***Figure 5**: Change in the proportion of subplots where shrubs were detected, from 1970 to 2017, by number of times burned.*

Soil moisture

There was variability in spatially-distributed soil moisture measurements in SCB, both among vegetation types and to a lesser degree among site visits (Figure 6). Specifically, soil moisture in dense meadows was approximately 3 times higher than in the other vegetation types, which were generally similar to each other (Figure 6). Furthermore, soil moisture in 2017 was higher than in 2016 or in 2018 across all vegetation types (Figure 6), consistent with measurements that 2017 was the wettest year of the three at our study site and in the southern Sierra Nevada in general (Table 1). There was more within-year variability during the drier 2016 water year (WY), with summer dry-down more evident than in the wetter 2017 WY (Figure 6) despite July measurements being taken on the same dates each year.

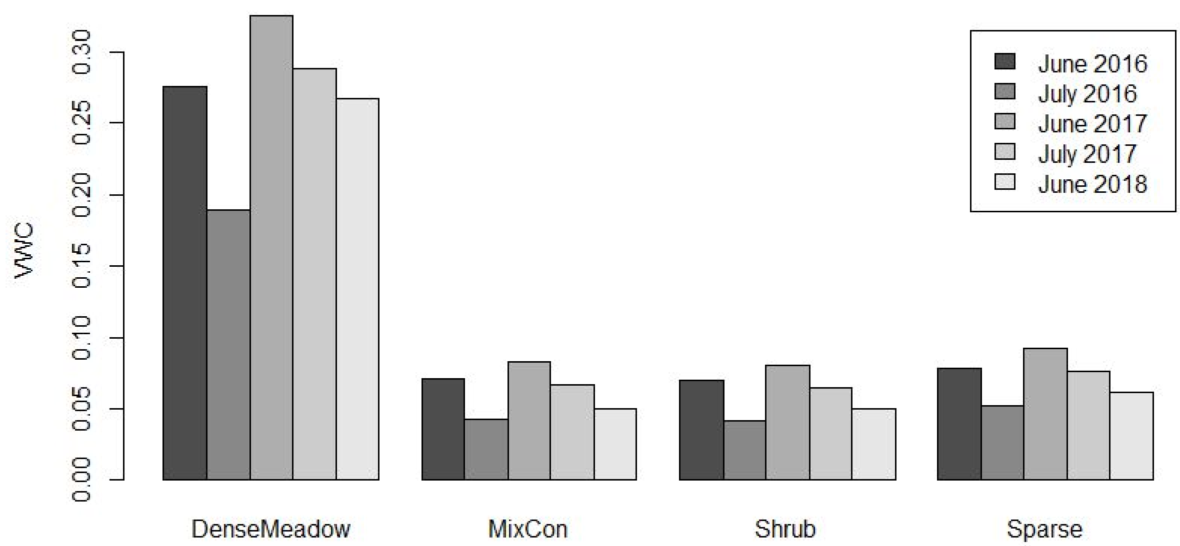

Figure 6*. Modeled mean soil moisture (volumetric water content; VWC) under each vegetation type and either June or July of each measurement year. The average is taken across all measurement points. Averaging across site means gives similar results, but with smaller magnitudes of variation between years.*

***Table 1**: Weather station data from Sugarloaf Creek Basin (SCB) and Illilouette Creek Basin (ICB). Gap-filled precipitation totals measured by rain gauge; cumulative shallow soil water gain was calculated from shallow soil moisture timeseries (Appendix B). End of water year (WY) deep soil moisture (Volumetric Water Content [VWC]) and number of saturation days were based on the 100 cm soil moisture probe record. Pearson's correlation coefficient was calculated between daily average 12 cm and 100 cm soil moisture for months of June - August.*

Weather Station	Vegetation Type	Total precipitation [mm]		Cumulative shallow (12-60 cm) soil water gain [mm]		End of WY VWC [%] at 100 cm		Days Saturated at 100 cm		Correlation coeff. between 12 & 100 cm VWC for Jun-Aug	
	WY:	**2017**	**2018**	**2017**	**2018**	**2017**	**2018**	**2017**	**2018**	**2017**	**2018**
SCB	Wetland	673	429	473	469	34	14	155	81	0.85	0.97
ICB	Wetland	1102	536	56	30	43	43	365*	365	0.88	0.54
SCB	Shrub	849	546	362	287	16	10	88	0	0.93	0.67
ICB	Shrub	1151	590	940	378	10	5.6	86*	0	0.87	0.84
SCB	Forest	599	393	834	184	4.7	3.4	56	0	0.99	0.97
ICB	Forest	768	456	776	334	3.5	3.4	31*	0	0.90	0.87

** :Approximated due to missing data as a result of the Empire Fire*

A random forest model fit to the measured soil moisture was able to predict the data with an RMSE of 3.6 and a Pearson correlation coefficient of 0.98. We tested the model's ability to extrapolate beyond training data: on average, when the model was trained on only 70% of the measured locations, it was able to predict soil moisture at the remaining 30% of locations with an RMSE of 10 and a correlation of 0.82. The relationship between soil moisture and site properties was similar for ICB and SCB, but not identical. In both watersheds, current vegetation type was the most important predictor of soil moisture (Appendix D; Figure D1). The random forest model trained on ICB measurements fit the measured SCB soil moisture measurements with a correlation coefficient of 0.73 (0.82 for site means), whereas the model fit to SCB data was able to predict them with a correlation of 0.98 (Figures D4, D5).

The random forest model showed small, but generally positive, changes in modeled June soil moisture as a result of fire (Figure 7). These results did not vary with year, but changes were slightly greater earlier in June compared to July or August (data not shown). The largest modeled changes in volumetric water content were less than 0.05, whereas in ICB a similar model predicted fire-related changes of up to 0.3 (Boisramé et al. 2018). Figure 7 also suggests that all areas that transitioned from conifer to dense meadow already had relatively high soil moisture prior to fire, and areas where forests encroached on meadows were relatively dry areas of meadow.

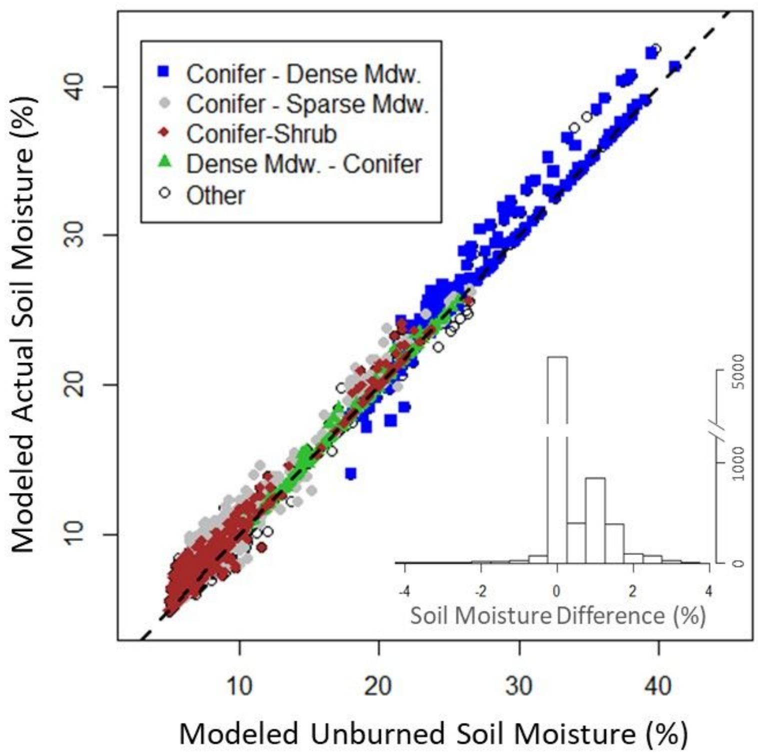

***Figure** 7. Modeled actual soil moisture (current vegetation cover and fire history) compared to modeled soil moisture assuming the same climatology (date set to early June) but no fire or vegetation change since 1973. The inset shows a histogram of the point-wise differences between these two sets of modeled values. Only locations where vegetation type changed between 1973 and 2014 are shown (see Figure 2). Locations that transitioned from conifer to dense meadow (mdw.) are shown as blue squares, conifer to sparse meadow as grey circles, conifer to shrub as red diamonds, and dense meadow to conifer as green triangles. Other types of transitions are rare (open black circles). Points above the dashed one-to-one line represent locations where the model predicts soil moisture is higher than it would have been without fire (positive numbers in the inset histogram).*

Consistent with the data from spatially-distributed soil moisture measurements (Figure 6), continuous weather station records (Figure 8; Appendix B) indicated that the wetland site was associated with the highest soil moisture among the three weather stations, followed by the shrub and forest sites, at all three soil depths measured (12, 60, and 100 cm). All sites experienced greater and more persistent soil moisture during the 2017 WY than the 2018 WY, as a result of large precipitation differences (SCB weather stations were installed in September 2016 at the end of the 2016 WY, so data were not available for that period). The forest stations tended to measure the least amount of precipitation (Table 1) and experience the earliest snowmelt (Figure B2), and had the greatest interannual soil moisture differences (Figure 8).

Cumulative shallow soil water gain showed idiosyncratic trends among sites and years (Table 1). At SCB, cumulative soil moisture gain was greatest at the forest site in 2017 but at the wetland site in 2018 (Table 1). Soil moisture gain at the forest site may be explained by rapid wetting and drying during the snowmelt period in 2017 (Figure 8), possibly due to relatively shallow snowpack experiencing diurnal fluctuations in freezing and thawing. Low values of cumulative soil moisture gain may also be attributable to saturation at certain sites. During the wet 2017 WY, all sites were saturated at 1-meter depth for some period of the year, yet during the drier 2018 WY, only soils at wetland stations experienced saturation. In ICB, the wetland site remained fully saturated for both 2017 and 2018 WYs, while in SCB the wetland site was saturated only for a portion of each year (Table 1). In general, deeper soils contained more water and were saturated longer than shallow soils, while shallow soil moisture was more responsive to precipitation, though water input pulses were apparent at 60 and 100 cm depths as well (Figure 8). Very shallow (12 cm) soil moisture was positively correlated with deep (100 cm) soil moisture (Table 1). Soil type and texture at the two sites were generally similar (Appendix B).

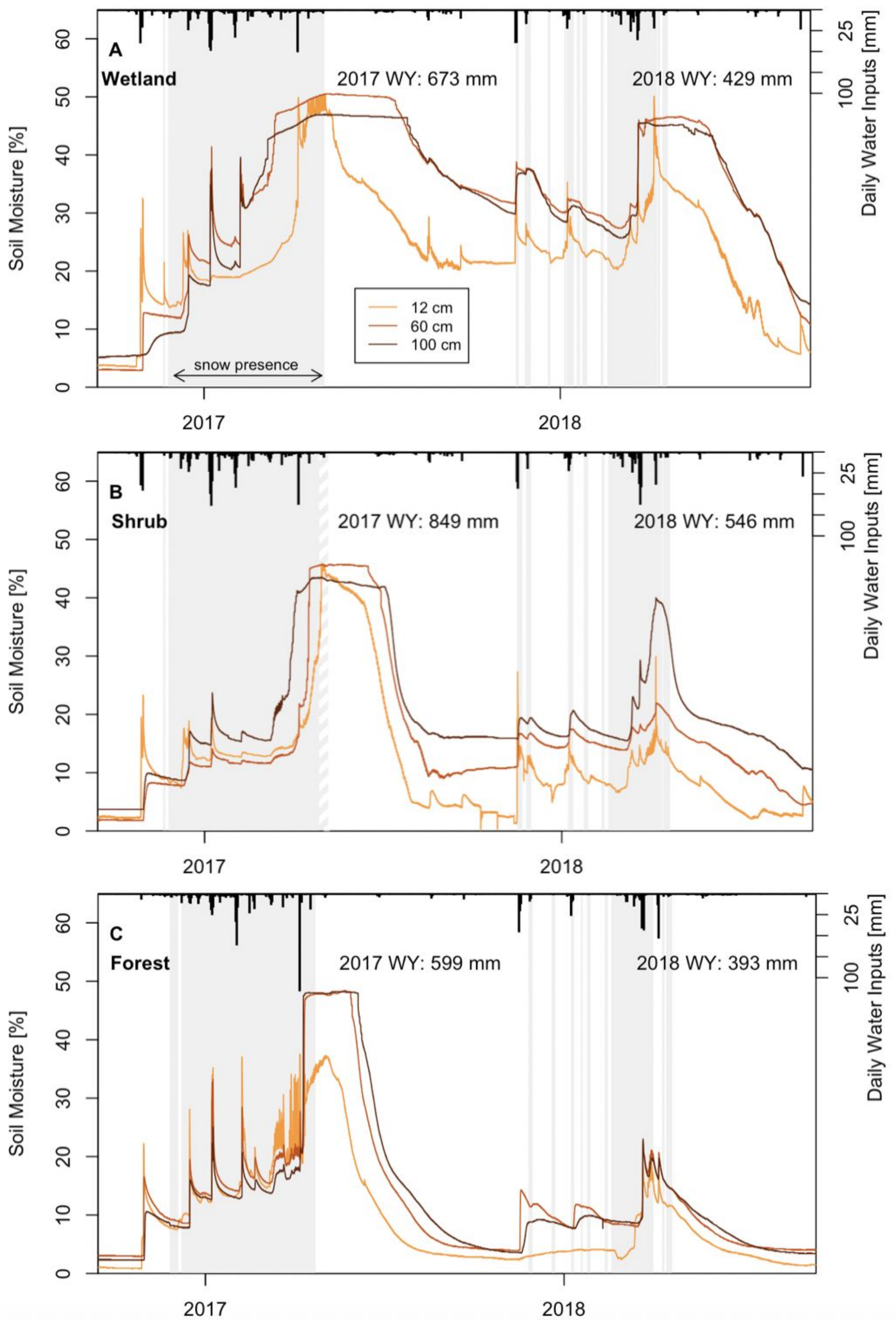

Figure 8: *Volumetric water content [%] in shallow (12 cm), mid (60 cm), and deep (100 cm) soils as measured by weather stations located in dense meadow (a), shrub (b), and forest (c) sites. Data were measured at 10 minute intervals for 2017 and 2018 water years. Vertical bars at top of panels indicate daily water inputs in the form of rain and snow melt. Grey regions represent periods of time when snow is present around the base of the weather station (at the shrub station camera data were not available in spring 2017, shown by grey hatching). Water year (WY) summaries are also provided for total water inputs recorded at each station. Refer to Appendix B for visuals of each site.*

Discussion

Fire-driven changes in dominant vegetation type (from aerial imagery analysis) and forest structure (from forestry plot data) were minimal at Sugarloaf Creek Basin (SCB), despite over 40 years of managed wildfire and ten fires greater than 40 ha over that time period in the basin. Although there was a slight increase in landscape heterogeneity and in sparse meadow cover over the 40 year period at SCB, the minimal changes in dominant vegetation type overall are a notable contrast from the nearby Illilouette Creek Basin (ICB), which had a similar duration of a restored semi-natural fire regime (Boisramé et al. 2017, Boisramé et al. 2017b, Boisramé et al. 2018). A number of potential explanations for this discrepancy exist, including differences in the fire history of the two basins, and differences in water balance and vegetation productivity between the two basins.

Approximately 5,500 ha (44%) of the 12,500 ha watershed burned at least once and approximately 1,300 ha (10%) of the watershed burned at least twice since 1973. Fires were slightly more active in ICB, with 52% of the ICB burning at least once in the same period, and 25% burning at least twice. Despite a marked increase over the fire suppression period, and over much of the Sierra Nevada outside of SCB and ICB (Mallek et al. 2013), this area burned may represent a relative lack of fire compared to an expected historical fire return interval over this period, as a relatively small fraction of the watershed (10%) received multiple fires given the pre-suppression fire return interval of ~9 years in this watershed (Collins and Stephens 2007). In particular, only 28 ha has burned in the SCB since 2004, with 59% of active ignitions suppressed, compared with 12,141 ha burned and only 23% of ignitions suppressed between 1969 and 2004 (A. Caprio, personal communication). This recent increase in fire suppression suggests that additional changes in vegetation cover and forest structure may have been observed had a historical fire return interval been more closely approximated.

The fires that burned in SCB were also predominantly low-intensity fires, due in part to the range of acceptable fire management conditions. Two of the most recent fires in SCB, the 1997 Sugarloaf Fire and the 2003 Williams Fire, were responsible for the bulk of the larger patches of overstory tree mortality that we detected in our vegetation change analysis (Figure 2). These two fires are also in a database of fire weather indices that enable comparison to 475 other fires across California in similar mixed-conifer and fir forest (Stevens et al. 2017). For maximum high temperature during the burn window, which was the number one climatic predictor of burn severity in this database (Stevens et al. 2017), the Williams Fire was in the 9^{th} percentile (23.4^{o}C) and the Sugarloaf Fire was in the 4^{th} percentile (21.7^{o}C).

SCB had a similar relative proportion of each vegetation type as ICB (Figure D6), and the two landscapes also had similar Shannon's Evenness Index and fractal dimension values in their pre-fire/post-suppression states (Figures D1, D5), but the maximum patch size of areas converted from forest to non-forest was higher in ICB (Figure D3). For larger high-severity patches to develop, there needs to be a confluence of weather and fuels sufficient to cause complete tree mortality (Collins et al. 2007). Relatively small patches of alternative vegetation are one of the primary goals of managed wildfire (Hessburg et al. 2016), so in that respect the fires within SCB may have met some management objectives with respect to the fine-scale heterogeneity on the landscape to improve resilience to future fires.

While weather conditions for many SCB fires may have been moderate, it is also possible that there was reduced fuel accumulation in SCB relative to ICB in the fire-suppression period, potentially due to lower precipitation and productivity in SCB. Three lines of evidence support wetter conditions in ICB vs SCB: first, streamflow standardized to area is greater in ICB and its encompassing watersheds (Table A2); second, interpolated /gridded precipitation data from

PRISM show higher annual precipitation in ICB (Table B2); and third, in-situ weather station data show higher annual precipitation in ICB (Table 1). Besides reducing productivity, drier conditions may make the SCB less hydrologically-responsive to wildfire-induced changes. For example, Roche et al. (2018) found that the Kings Watershed had less post-fire reductions in ET than the American River Watershed, which had higher precipitation and greater post-fire basal area.

Beyond the relatively modest creation of alternative vegetation patches following fire-caused overstory tree mortality (Figure 3), we did not observe the expected changes in forest structure from our re-measurement of forestry plots (Figure 4) that we would have expected under managed wildfire (Larson et al. 2013). Specifically, we observed a slight increase in tree density in all burn classes that was concentrated in the smallest size class (7.6 – 15.2 cm; Figure 4a). One of the objectives of managed wildfire is the removal of smaller understory trees, particularly of fire-sensitive species (North et al. 2012, North et al. 2015), an outcome that has been observed with managed wildfire in other wilderness areas (Larson et al. 2013). However in SCB, even in twice-burned plots, we saw an increase in fire sensitive species (e.g. *Pinus contorta*) in smaller size classes (Figure 4c). The four plots that burned twice were all in areas that did not map as alternative vegetation types, so the burns were likely low severity in those areas (Figure 1, 2), if they burned at all (recognizing that managed wildfires are inherently patchy due to variation in surface fuels). Furthermore, two of the four twice-burned plots burned in the 2003 Williams fire while the other two had not burned since the 1985 Sugarloaf fire. Given the absence of recent fire in the watershed discussed above (A. Caprio, pers. comm.; Table A1), it is conceivable, even likely, that the regeneration we observed in the smallest size class (Figure 4a) has filled in since the fires of the 1980's and late 1990's, highlighting the

555 importance of repeated fires to continue to regulate fuels and the spatial heterogeneity of fire-
556 prone forests (North et al. 2012).

557 The data from the forestry plots also revealed that fire occurrence is not uniform across
558 vegetation types. We detected an increased fire probability in plots that had previously been
559 dominated by Jeffrey pine (*Pinus jeffreyi*), and to a lesser extent, white fir (*Abies concolor*), and
560 a lower probability in red fir (*Abies magnifica*) forest. This is expected given the historical fire
561 regimes and fire frequencies of these two vegetation types (Steel et al. 2015, Safford and Stevens
562 2017), with red fir forests generally having a less conducive climate for fire spread, and a less-
563 flammable fuel bed. Thus, we would not necessarily expect similar fire effects on vegetation
564 across the entire watershed. However, an unexpected observation from the forestry plot data was
565 the uniform decrease in large (>61 cm) and very large (>100 cm) trees, even in unburned red fir
566 forest (Figure 4). This is consistent with long-term trends that have been observed across the
567 western US (van Mantgem and Stephenson 2007, van Mantgem et al. 2009, Das et al. 2016), and
568 may be indicative of climate or pest/pathogen influences in addition to fire. For instance, the US
569 Forest Service Aerial Detection Monitoring program detected tree mortality from both mountain
570 pine beetle (*Dendroctonus ponderosae*) and fir engraver (*Scolytus ventralis*) within SCB in 2015
571 (Moore et al. 2015). Prominent decreases in large and very large trees were observed in *Pinus*
572 *jeffreyi* (Figure 4i, l), which is the most fire-resistant species in SCB (Stevens unpublished data),
573 suggesting that fire may not be the agent of mortality in this size class, even in twice-burned
574 forestry plots.

575 The lack of a strong watershed-wide signal of changing soil moisture is due to both the
576 relatively low initial abundance and minimal post-fire expansion of the dense meadow vegetation
577 class, and to minimal detectable differences between forest, shrub, and dry meadow soil moisture

profiles. Both of these factors could be attributable to soil and topographic properties of the watershed as well as precipitation and productivity effects as discussed above. Consequently, we do not predict large changes in soil moisture at the watershed scale in association with the managed fire regime. We note that the vegetation changes we observed were primarily transitions from mixed-conifer to shrub, mixed-conifer to sparse meadow, or shrub to sparse meadow (Figure 2, 3), with minimal transition to the vegetation type that would be expected to have the greatest change on soil moisture, namely dense meadows (Figure 7). This stands in contrast to the more productive ICB (Appendix B), where pronounced increases in the dense meadow vegetation type were observed following fire (Boisramé et al. 2017, Boisramé et al. 2017b). In addition, the minimal changes to forest structure following fire (discussed above) may partially account for fire history variables having very small impacts on soil moisture independent of vegetation change (Figure D3). If forests had generally become much more open, or dominated by different sizes or species of trees following fire, we might expect greater impacts of fire on soil moisture within forested plots. For example, the "shrub" weather station is dominated by small conifers, while the forest station is dominated by large conifers, and soil moisture was higher in the "shrub" station for most of the data record (Figure 8).

In ICB, there may have been a greater encroachment of trees, particularly lodgepole pine, into meadows during the early 19th century fire exclusion period. This higher encroachment could be due to the ICB's higher productivity relative to SCB, greater consistency in soil saturation of the SCB meadows (this limiting conifer growth), or a combination of both. The managed fire program at ICB could consequently have had a greater restorative effect in areas of meadow encroachment than at SCB. We observed fire-caused tree mortality adjacent to several pre-existing dense meadows at SCB, and yet there was very little expansion of dense meadows into these areas, which instead typically transitioned to sparse meadows (Figure 2, 3). This suggests that climate, topography and soil type may be constraining meadow locations at SCB more than at ICB, and the potential gain in soil moisture and herbaceous vegetation following forest removal by managed wildfire may therefore be low at SCB.

High correlations between shallow and deep soil moisture during summer months (Table 1) show that our spatially-distributed soil moisture measurements provide a reasonable representation of spatial patterns in deeper soil moisture. However, this correlation only captures relative changes over time, not absolute values. In late summer, there was a greater difference between deep and shallow soil moisture at the shrub and wetland stations than there was at the forest station (Figure 8). Therefore, it is possible that transitions from mature forest to more open vegetation cover might lead to greater increases in deeper soil moisture than would be suggested by shallow soil moisture. This could mean that the modeled surface soil moisture changes in Figure 8 may underestimate the total change in plant-available moisture. Findings from the ICB also suggested that the soil moisture impact of forest removal might be larger in deeper soils (Boisramé et al. 2018).

Similarities in the random forest models trained on ICB and SCB moisture data show that certain variables are consistently strong predictors of soil moisture. For example, vegetation cover type and TWI were within the top 4 most important predictors of soil moisture for both ICB and SCB, with years since fire, times burned, and year of measurement being the least important predictors in both watersheds (Figures C1 and C1b). However, the relatively poor ability of the ICB-trained model to predict SCB moisture values indicates that the relative importance of these factors for controlling summer soil moisture varies between the watersheds. The extent to which this variation should be attributed to physical and ecological factors in the watershed, and the extent to which it reflects features of the random forest methodology is not clear.

Large observed differences in precipitation, snowpack depth and melt timing between the three weather stations suggest that vegetation transitions in the SCB could induce important differences in the quantity and timing of water input to the soil. For instance, we observed increased snowpack depth and duration in relatively small high-severity patches at SCB (Appendix B; Figure B3). This contrasts to other observations (made during a low snowpack year) which showed reduced snowpack depth associated with larger patches of high-severity fire (Stevens 2017). Despite the differences in snowpack and melt timing between vegetation types, distributed soil moisture measurements showed only relatively small differences in summer soil moisture between forest, shrub, and sparse meadow vegetation classes (Figures 6, D3). The sandy soils and relatively modest cumulative precipitation in the SCB may result in rapid drainage of the soil profiles and a tendency for water-limited conditions in the basin. These conditions could limit how the apparent effects of vegetation on snowpack volume and snowmelt timing translate to eventual summer soil moisture. Sparse meadows and shrub vegetation may also be located in generally drier areas (e.g., high sun exposure, steep slopes, and well-drained soils), where increases in water inputs due to reduced forest cover may not be evident. Although the weather stations do show wetter surface soils where water inputs were greater (shrub and wetland; Figure 8), some of this increased moisture could be due to slight differences in slope at each station (13 degrees at the forest station, 8 degrees at the shrub station, and 4 degrees at the wetland station). Future work using data from these weather stations will explore the relationships between land cover, precipitation, snowpack, and soil moisture in greater detail.

647 Conclusion

648 Our characterization of vegetation change and the hydrological response following the
649 implementation of a natural fire program in SCB demonstrates the contextual nature of
650 landscape-level fire-ecosystem interactions. If, in the absence of local historical imagery and on-
651 the-ground forest structure data, we were to predict fire-related changes in SCB using findings
652 from a similar study conducted in ICB, we would have overestimated fire-driven change in
653 vegetation and in water availability. While the direction of change and predictors of soil moisture
654 were similar for the two watersheds, the magnitude of change was much lower in SCB. This
655 discrepancy appears to be due to the interaction between watershed-level productivity and fire
656 effects. In SCB the lower overall productivity and the lesser proportions of high severity fire
657 effects relative to ICB led to greater stability in vegetation over time and a more muted
658 hydrological response to managed wildfire in SCB. More landscape-level experimentation in
659 other watershed, including lower elevation sites, would be needed to better elucidate the drivers
660 of landscape and hydrologic change in response to natural fire regimes.

661 Acknowledgments

662 Field work assistance was provided by K. Collins, M. Goering, J. Levine, L. Nitsan, C. Phillips,
663 and A. Welsh. Imagery analysis assistance was provided by J. Ngyuen, L. Nitsan, and S. Tang.
664 A. C. Caprio provided helpful information on the managed fire program at Sequoia Kings
665 Canyon National Park. This work was supported by the U.S. Joint Fire Science Program (grant
666 number 14-1-06-22); the National Science Foundation EAR (grant number 1013339); Sigma Xi
667 Grants in Aid of Research; the UC Berkeley SMART program; the Hellman Fellows Program;
668 the UC Agriculture and Natural Resources competitive grant program; and the UC Berkeley
669 Philomathia Graduate Fellowship in Environmental Sciences.

Literature Cited

Bales, R. C., J. W. Hopmans, A. T. O'Geen, M. Meadows, P. C. Hartsough, P. Kirchner, C. T. Hunsaker, and D. Beaudette. 2011. Soil moisture response to snowmelt and rainfall in a Sierra Nevada mixed-conifer forest. Vadose Zone Journal **10**:786-799.

Bates, D. M., M. Maechler, B. M. Bolker, and S. Walker. 2013. lme4: Linear mixed-effects models using Eigen and S4. R package version 1.0-5. CRAN.R-project.org/package=lme4.

Blaschke, T., G. J. Hay, M. Kelly, S. Lang, P. Hofmann, E. Addink, R. Q. Feitosa, F. Van der Meer, H. Van der Werff, F. J. I. j. o. p. Van Coillie, and r. sensing. 2014. Geographic object-based image analysis–towards a new paradigm. **87**:180-191.

Boisramé, G., S. Thompson, B. Collins, and S. Stephens. 2017. Managed wildfire effects on forest resilience and water in the Sierra Nevada. Ecosystems **20**:717–732.

Boisramé, G., S. Thompson, and S. Stephens. 2018. Hydrologic responses to restored wildfire regimes revealed by soil moisture-vegetation relationships. Advances in Water Resources **112**:124-146.

Boisramé, G. F. S., S. E. Thompson, M. Kelly, J. Cavalli, K. M. Wilkin, and S. L. Stephens. 2017b. Vegetation change during 40years of repeated managed wildfires in the Sierra Nevada, California. Forest Ecology and Management **402**:241-252.

CalFire. 2018a. Top 20 largest California wildfires. http://www.fire.ca.gov/communications/downloads/fact_sheets/Top20_Acres.pdf.

CalFire. 2018b. Top 20 most destructive California wildfires. http://www.fire.ca.gov/communications/downloads/fact_sheets/Top20_Acres.pdf.

Caprio, A. C., and D. M. Graber. 2000. Returning fire to the mountains: can we successfully restore the ecological role of pre-Euroamerican fire regimes to the Sierra Nevada?*in* In:

694 Cole, David N.; McCool, Stephen F.; Borrie, William T.; O'Loughlin, Jennifer, comps.
695 2000. Wilderness science in a time of change conference-Volume 5: Wilderness ecosystems,
696 threats, and management; 1999 May 23–27; Missoula, MT. Proceedings RMRS-P-15-VOL-
697 5. Ogden, UT: US Department of Agriculture, Forest Service, Rocky Mountain Research
698 Station. p. 233-241.
699 Collins, B. M., R. G. Everett, and S. L. Stephens. 2011. Impacts of fire exclusion and recent
700 managed fire on forest structure in old growth Sierra Nevada mixed-conifer forests.
701 Ecosphere **2**:art51.
702 Collins, B. M., M. Kelly, J. W. van Wagtendonk, and S. L. Stephens. 2007. Spatial patterns of
703 large natural fires in Sierra Nevada wilderness areas. Landscape Ecology **22**:545-557.
704 Collins, B. M., J. M. Lydersen, D. L. Fry, K. Wilkin, T. Moody, and S. L. Stephens. 2016.
705 Variability in vegetation and surface fuels across mixed-conifer-dominated landscapes with
706 over 40 years of natural fire. Forest Ecology and Management **381**:74-83.
707 Collins, B. M., J. D. Miller, A. E. Thode, M. Kelly, J. W. van Wagtendonk, and S. L. Stephens.
708 2009. Interactions among wildland fires in a long-established Sierra Nevada natural fire
709 area. Ecosystems **12**:114-128.
710 Collins, B. M., and S. L. Stephens. 2007. Managing natural wildfires in Sierra Nevada
711 wilderness areas. Frontiers in Ecology and the Environment **5**:523-527.
712 Das, A. J., N. L. Stephenson, and K. P. Davis. 2016. Why do trees die? Characterizing the
713 drivers of background tree mortality. Ecology **97**:2616-2627.
714 FRAP. 2017. Fire and Resource Assessment Program. Fire perimeters [Database]. Sacramento,
715 CA: California Department of Forestry and Fire Protection. Available from:

http://frap.fire.ca.gov/data/frapgisdata-sw-fireperimeters_download; last accessed 13-March_2019.

Grant, G. E., C. L. Tague, and C. D. Allen. 2013. Watering the forest for the trees: an emerging priority for managing water in forest landscapes. Frontiers in Ecology and the Environment **11**:314-321.

Halekoh, U., and S. Højsgaard. 2014. A Kenward-Roger Approximation and Parametric Bootstrap Methods for Tests in Linear Mixed Models - The R Package pbkrtest. Journal of Statistical Software **59**:1-30.

Hessburg, P. F., T. A. Spies, D. A. Perry, C. N. Skinner, A. H. Taylor, P. M. Brown, S. L. Stephens, A. J. Larson, D. J. Churchill, N. A. Povak, P. H. Singleton, B. McComb, W. J. Zielinski, B. M. Collins, R. B. Salter, J. J. Keane, J. F. Franklin, and G. Riegel. 2016. Tamm Review: Management of mixed-severity fire regime forests in Oregon, Washington, and Northern California. Forest Ecology and Management **366**:221-250.

Larson, A. J., R. T. Belote, C. A. Cansler, S. A. Parks, and M. Dietz. 2013. Latent Resilience in Ponderosa Pine Forest: Effects of Resumed Frequent Fire. Ecological Applications.

Liaw, A., and M. J. R. n. Wiener. 2002. Classification and regression by randomForest. **2**:18-22.

Little, R. J. A. 1988. Missing-data adjustments in large surveys. Journal of Business & Economic Statistics **6**:287-296.

Mallek, C., H. Safford, J. Viers, and J. Miller. 2013. Modern departures in fire severity and area vary by forest type, Sierra Nevada and southern Cascades, California, USA. Ecosphere **4**:art153.

McGarigal, K., S. A. Cushman, and E. J. C. s. p. p. b. t. a. a. t. U. o. M. Ene, Amherst. Available at the following web site: http://www. umass. edu/landeco/research/fragstats/fragstats. html.

739 2012. FRAGSTATS v4: spatial pattern analysis program for categorical and continuous maps.

741 McKelvey, K. S., C. N. Skinner, C. Chang, D. C. Erman, S. J. Hussari, D. J. Parsons, J. W. van Wagtendonk, and C. P. Weatherspoon. 1996. An overview of fire in the Sierra Nevada., University of California, Centers for Water and Wildland Resources, Davis, CA.

744 Miller, J. D., E. E. Knapp, C. H. Key, C. N. Skinner, C. J. Isbell, R. M. Creasy, and J. W. Sherlock. 2009. Calibration and validation of the relative differenced Normalized Burn Ratio (RdNBR) to three measures of fire severity in the Sierra Nevada and Klamath Mountains, California, USA. Remote Sensing of Environment **113**:645-656.

748 Moore, J., Z. Heath, and B. J. F. S. T. r. U. S. D. o. A. Bulaon. 2015. Aerial detection survey-April 15th-17th, 2015.

750 North, M., B. M. Collins, and S. Stephens. 2012. Using fire to increase the scale, benefits, and future maintenance of fuels treatments. Journal of Forestry **110**:392-401.

752 North, M. P., S. L. Stephens, B. M. Collins, J. K. Agee, G. Aplet, J. F. Franklin, and P. Z. Fulé. 2015. Reform forest fire management. Science **349**:1280-1281.

754 Parks, S. A., L. M. Holsinger, C. Miller, and C. R. Nelson. 2015. Wildland fire as a self-regulating mechanism: the role of previous burns and weather in limiting fire progression. Ecological Applications **25**:1478-1492.

757 Ponisio, L. C., K. Wilkin, L. K. M'Gonigle, K. Kulhanek, L. Cook, R. Thorp, T. Griswold, and C. Kremen. 2016. Pyrodiversity begets plant–pollinator community diversity. Global Change Biology:n/a-n/a.

Roche, J. W., M. L. Goulden, and R. C. Bales. 2018. Estimating evapotranspiration change due to forest treatment and fire at the basin scale in the Sierra Nevada, California. Ecohydrology **11**:e1978.

Safford, H. D., and J. T. Stevens. 2017. Natural Range of Variation (NRV) for yellow pine and mixed conifer forests in the Sierra Nevada, southern Cascades, and Modoc and Inyo National Forests, California, USA. USDA Forest Service, Pacific Southwest Research Station. General Technical Report PSW-GTR-256, Albany, CA.

Steel, Z. L., H. D. Safford, and J. H. Viers. 2015. The fire frequency-severity relationship and the legacy of fire suppression in California forests. Ecosphere **6**:art8.

Stephens, S. L., J. K. Agee, P. Z. Fulé, M. P. North, W. H. Romme, T. W. Swetnam, and M. G. Turner. 2013. Managing forests and fire in changing climates. Science **342**:41-42.

Stephens, S. L., B. M. Collins, E. Biber, and P. Z. Fulé. 2016. U.S. federal fire and forest policy: emphasizing resilience in dry forests. Ecosphere **7**:e01584-n/a.

Stephenson, N. L. 1998. Actual evapotranspiration and deficit: biologically meaningful correlates of vegetation distribution across spatial scales. Journal of Biogeography **25**:855-870.

Stevens, J. T. 2017. Scale-dependent effects of post-fire canopy cover on snowpack depth in montane coniferous forests. Ecological Applications **27**:1888-1900.

Stevens, J. T., B. M. Collins, J. D. Miller, M. P. North, and S. L. Stephens. 2017. Changing spatial patterns of stand-replacing fire in California conifer forests. Forest Ecology and Management **406**:28-36.

van Mantgem, P. J., and N. L. Stephenson. 2007. Apparent climatically induced increase of tree mortality rates in a temperate forest. Ecology Letters **10**:909-916.

van Mantgem, P. J., N. L. Stephenson, J. C. Byrne, L. D. Daniels, J. F. Franklin, P. Z. Fulé, M. E. Harmon, A. J. Larson, J. M. Smith, A. H. Taylor, and T. T. Veblen. 2009. Widespread increase of tree mortality rates in the western United States. Science **323**:521-524.

van Wagtendonk, J. W. 2007. The history and evolution of wildland fire use. Fire Ecology **3**:3-17.

Westerling, A. L., and T. W. J. E. Swetnam, Transactions American Geophysical Union. 2003. Interannual to decadal drought and wildfire in the western United States. EOS, Transactions American Geophysical Union **84**:545-555.

Appendix A: Sugarloaf Creek Basin Site Information

Table A1. All fires from FRAP (2017) perimeter database the burned within SCB. Fires included in the analysis burned 57% of SCB.

Year	Name	Report date	Total area (ha)	Area of watershed burned (ha)	Included in analyses?
1952	Sugarloaf	19-Jun	15	15	
1964	Williams	2-Oct	5	5	
1971	Ball Dome	13-Aug	99	99	
1972	Sugar Valley	15-Sep	16	5	
1973	So. Sentinel	28-Aug	1084	1038	Y
1974	Comanche	22-Jul	1219	1219	Y
1976	In Between	29-Jul	13	13	Y
1977	Sugarloaf	20-Jul	264	264	Y
1977	Ferguson	26-Jun	4219	1594	Y
1980	Roaring	1-Aug	170	72	Y
1985	Sugarloaf	28-Jul	1153	1152	Y
1988	Sugarbaby	20-Jun	3	3	Y
1992	Ellis Meadow	2-Jun	23	23	Y
1997	Sugarloaf	15-Aug	114	114	Y
1999	Williams	18-Sep	232	232	Y
2003	Williams	28-Jul	1429	1427	Y
2004	Ferguson	7-Jul	1	1	
2006	Pond	13-Aug	5	0	

Table A2. Specific discharge (total streamflow volume divided by watershed area) from the Merced Watershed (which contains ICB) and South Fork Kings River Watershed (which contains SCB) illustrate drier conditions in the region including SCB. IRMA = irma.nps.gov/AQWebPortal

Large Watershed	**Sub-Watershed Measurement Point**	**Gage # or Data Source**	**Lat/Lon**	**Sub-watershed Area**	**Years**	**Mean Annual Specific Discharge (Flow/Area)**
South Fork Kings	SF Kings River Near Cedar Grove, CA	USGS 11212500	36°48’25” N 118°44’55” W	1056 km^2	1950-1957	0.55 m/yr
South Fork Kings	Kings River near Hume, CA	USGS 11213000	36°50’50” N 118°53’50” W	2160 km^2	1921-1958	0.48 m/yr
Merced	Illilouette Creek at Ill. Falls Bridge	*IRMA*	37°42’43” N 119°33’35” W	150 km^2	2011-2017	0.8 m/yr
Merced	Illilouette Creek at base of Illilouette Falls	Modeled (Boisramé et al. 2019, in press)	37°43’32” N 119°33’27” W	150 km^2	1972-2017	0.9 m/year
Merced	Merced River at Happy Isles Bridge nr Yosemite CA	USGS 11264500	37°43’53” N 119°33’33” W	469 km^2	1921-1958	0.66 m/yr
Merced	Merced River at Pohono Bridge nr Yosemite CA	USGS 11266500		831 km^2	1921-1958	0.65 m/yr

Appendix B: Sugarloaf Creek Basin and Illilouette Creek Basin weather station sites

We installed three temporary weather stations in Sugarloaf Creek Basin (SCB) in September 2016, with one weather station each in dense meadow, shrub, and mature mixed conifer vegetation types, and all sites located within 200m of each other. The dense meadow weather station site has dense grass cover with some conifer regeneration, but no overstory above the weather station. It is situated in an area that burned at high severity in 2003. The shrub weather station consists of whitethorn ceanothus (*Ceanothus cordulatus*) interspersed with grasses, some conifer regeneration, and no overstory above the station. The SCB shrub site also burned at high severity in 2003. The mixed conifer site has little herbaceous vegetation, and mature mixed conifers form the overstory. This site burned at low severity in 2003. Fire severity characterizations are based on remote sensing, aerial photography and visual observations of tree mortality at each site.

The weather stations generated incomplete precipitation records due to frozen tipping buckets, downtime for station maintenance, and damage by wildlife. Where possible, we gap-filled precipitation at one station using predictive mean matching (mice.impute.pmm function in R package "MICE") to perform multiple imputations of the missing data. Predictive mean matching (Little 1988) is an advantageous technique for large datasets having non-normal distributions, and discrete values with physical bounds (in our case precipitation cannot be less than zero). When all three stations were missing precipitation data we gap-filled using a combination of snowmelt (determined by decreases in snow depth, using an averaged density of 0.4 swe/snow depth), or observed increases in shallow soil water. All predictions were rounded to the nearest 0.1 inch (2.54 mm), the smallest increment in the rain gauge.

We compared soil moisture observations from the weather stations to the average of a spatially-distributed grid of local measurements made with the hand-held soil moisture meter (Table B1). Spatial averages were calculated from 25 measurements made in a 100 x 100 foot (30.48 m) grid centered on each weather station site, and compared to the 12 cm deep TDR at the weather stations. The consistency between the results indicates both that the weather stations were representative of their local area and that the mobile and in-situ instrumentation performed similarly. The slightly wetter measurements found at the weather stations are consistent with the differences in orientation between the measurements, with the manual measurements averaging soil water content vertically from the surface to the depth of 12 cm, and the buried moisture probes averaging soil water content horizontally at the depth of 12 cm.

To investigate another metric of relative water balance differences between the three vegetation sites, we calculated cumulative shallow soil moisture gain at each site, defined as the cumulative increase in shallow soil moisture over the duration of the study. We averaged the two soil moisture measurements at 12 cm and 60 cm depths ("shallow soil") at every 10-minute measurement interval, and then calculated a six-hour moving-window average soil moisture for each measurement interval using all measurements on three hours on either side of the target measurement interval to eliminate signal noise. An increase between two consecutive 10-minute average soil moisture records was considered to be water gain in the shallow soil column. To convert percent volumetric water content (VWC) measured by the probes to a depth of water accumulated at each time step, we multiplied the increase in VWC between two measurements by 48 cm (the depth of the shallow soil moisture column; decreases and zero values between intervals were ignored). Cumulative soil moisture gain is thus the sum of soil moisture gains for each individual 10-minute timestep over the course of the recorded water year.

Table B1. Comparison of spatially averaged (± 1 standard deviation) shallow soil moisture readings and the time averaged in-situ TDR soil moisture readings at 12cm at the SCB weather stations. In the late summer campaign, wetland and forest sites were measured on August 5th, and the shrub site on August 9th.

	May 23rd, 2017			**August 5th / 9th 2017**		
	Wetland	**Forest**	**Shrub**	**Wetland**	**Forest**	**Shrub**
Spatial average	48%±13%	8.7%±2.3%	7.5%±1.8%	41%±14%	1.3%±1.2%	1.0%±0.6%
12cm weather station	49%	11%	10%	49%	2.2%	2.9%

Soil samples were collected during installation of the soil moisture probes at each weather station, and analyzed for organic matter content as well as soil texture. Soils were loamy sand or sand at all sites and depths. Shallow wetland soils (top 10cm) in both ICB and SCB showing higher organic matter and silt content compared to both deeper wetland soils and all shrub/forest soils.

The vegetation at the weather stations at ICB was similar but not identical to SCB. The SCB wetland site contains larger portion of conifer regeneration than ICB, which is predominantly vegetated with tall grasses. The shrub site in ICB was comprised mostly of whitethorn ceanothus (*Ceanothus cordulatus*) when weather stations were installed, but burned at high severity during the 2017 Empire Fire, resulting in bare soil with little live vegetation during the 2018 WY. The SCB shrub site contains a dense growth of young conifers with a mix of ceanothus and grass. The forest sites in the two basins are similar in terms of tree density, tree species, and slope. Similar to ICB, soils at the SCB weather station sites were all loamy sand, with higher silt content in the meadow site than at the other two sites. Soil texture at both SCB and ICB did not vary greatly with depth, although the meadow site had higher organic content at shallow depths than the shrub and forest sites.

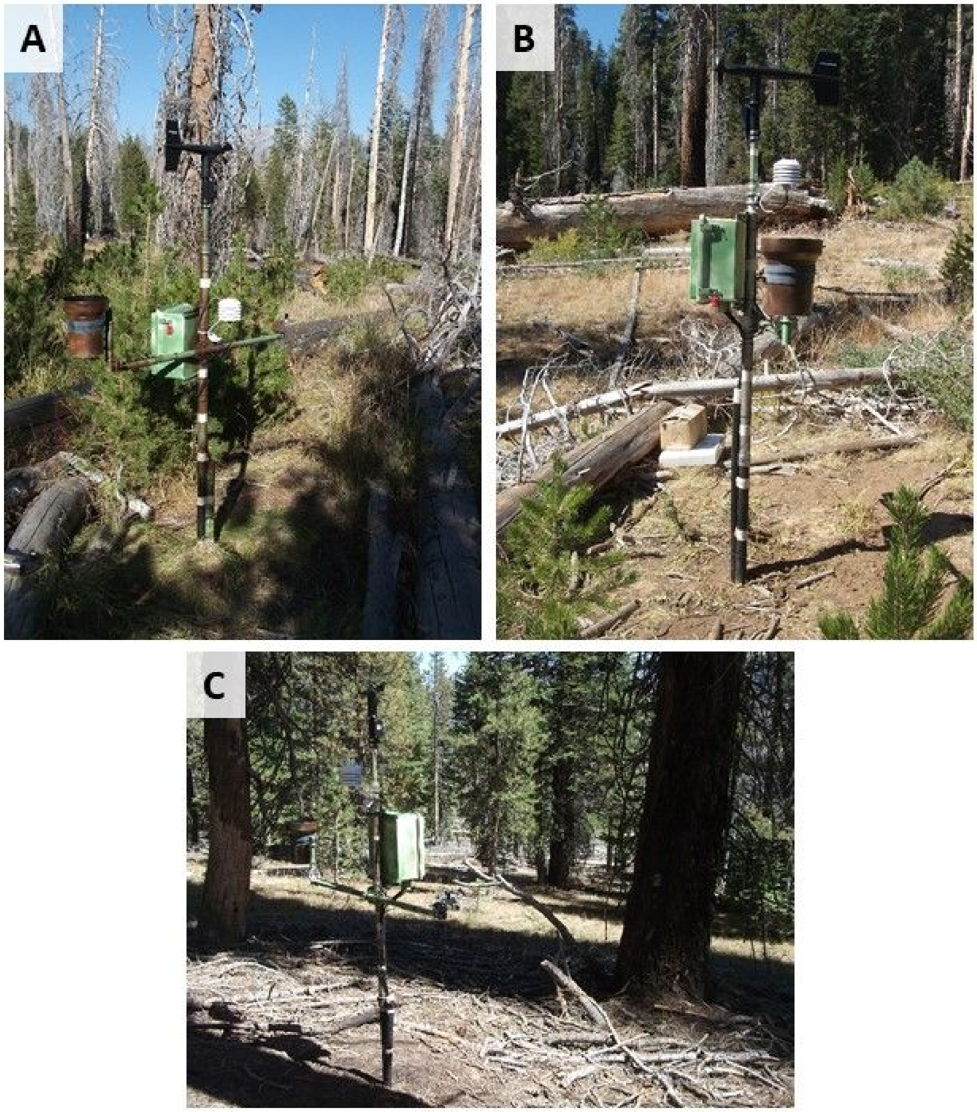

Figure B1: Images of weather stations in Sugarloaf Creek Basin. These stations are located in three nearby areas: one relatively wet site dominated by grasses and conifer recruitment (A; referred to as "wetland" in the main text), one drier site with sparse conifer recruitment and shrub growth (B; referred to as "shrub" in the main text), and one with an intact mature conifer canopy (C; referred to as "forest" in the main text).

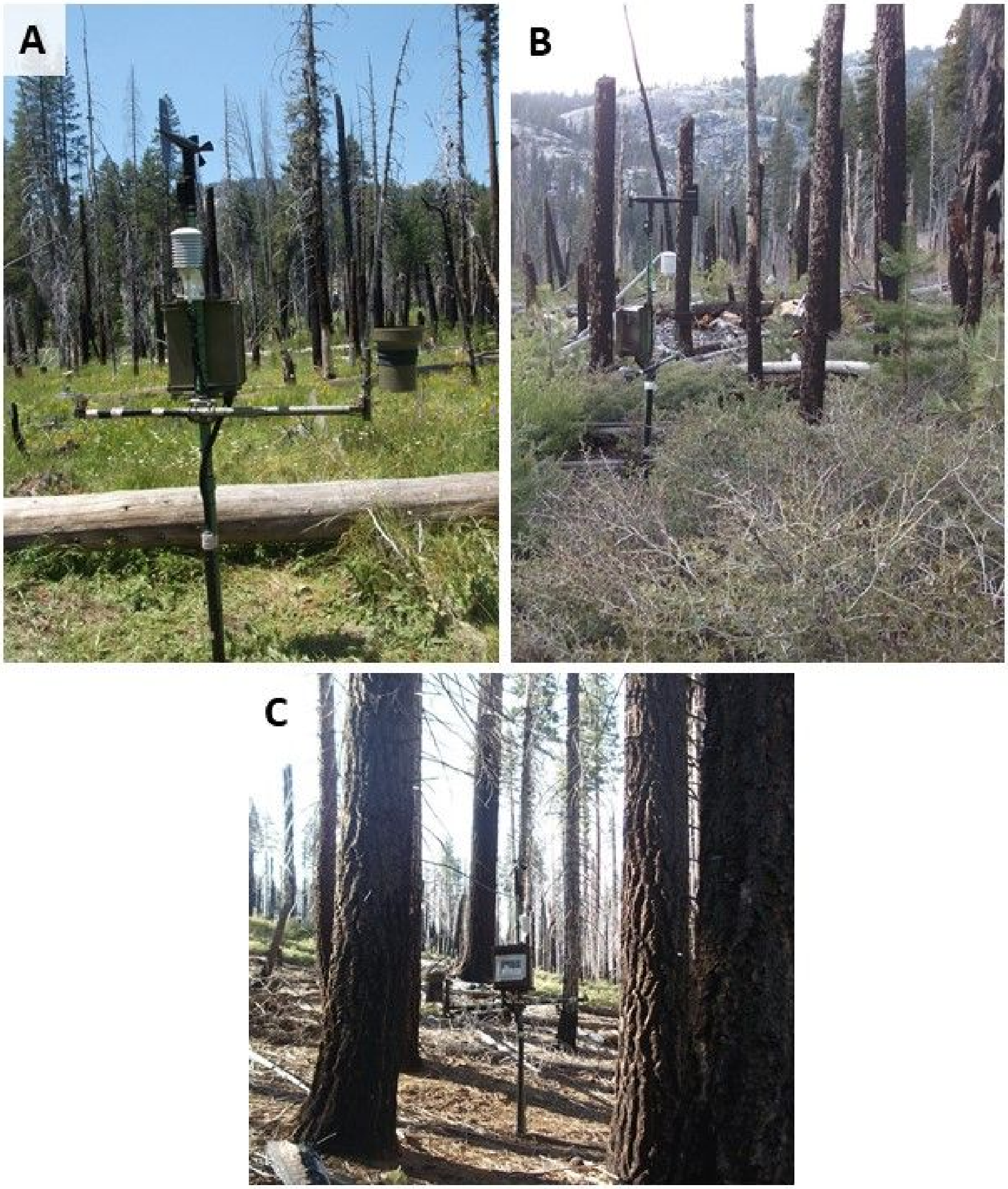

Figure B2: Images of weather stations in Illilouette Creek Basin. These sites are dominated by wetland vegetation (A; "wetland"), shrubs and conifer recruitment (B; "shrub"), and a mature conifer canopy (C; "forest").

95 The weather stations reported more precipitation in ICB than SCB (Table B2), with the differences being larger (1.3-1.6 times more precipitation in ICB than SCB) in 2017 (a wet year) than 2018 (1.1-1.2 times more precipitation in ICB), a dry year. Precipitation totals for ICB are conservative for 2017 WY because of the removal of the weather stations prior to the Empire Fire (September through the end of November 2017). At least two precipitation events occurred during this time. Comparing the weather station precipitation estimates to PRISM data (http://www.prism.oregonstate.edu) at the same locations shows the same general trends in space and time, giving us confidence in our estimates of the relative differences in precipitation between the basins, even if the exact values do not agree (Table B2). PRISM precipitation is highly uncertain in the Sierra Nevada, and the differences in annual total precipitation do not indicate that ICB/SCB measurements are erroneous (Henn et al. 2018).

Table B2. Annual precipitation estimates for water years (WY) 2016 through 2018. Weather station estimates are averaged between the non-forest stations at each watershed (ICB and SCB) as these stations should not experience interception losses. The ratio of precipitation between sites and between datasets show that for 2016-2018 ICB always received more annual precipitation than SCB (regardless of dataset), and PRISM always estimated higher precipitation than our weather stations.

	WY 2016	**WY 2017**	**WY 2018**
Weather Station, ICB	580 mm	1130 mm	560 mm
PRISM, ICB	1028 mm	2017 mm	797 mm
Weather Station, SCB	NA	780 mm	490 mm
PRISM, SCB	843 mm	1491 mm	673 mm
ICB/SCB, Weather Stations.	NA	1.45	1.14
ICB/SCB, PRISM	1.22	1.35	1.19
PRISM/Station, ICB	1.77	1.78	1.42
PRISM/Station, SCB	NA	1.96	1.37

Most precipitation in both basins is in the form of snow, and the basins had different snowpack depths (Figure B3). Snow data in 2017 are incomplete for SCB because of periods of time when the snowpack covered the cameras. Nonetheless, we estimate that snow depth was similar between the two sites during the 2017 and 2018 WYs. In ICB manual snow depth measurements were taken in a grid around each weather station in March 2016, January and April 2017, and March 2018 (points and error bars on Figure B2 for ICB), but manual measurements were not made at SCB because the site was inaccessible in the winter. For both locations and all water years, the wetland station had the greatest snowpack depth and the latest melt date, and the forest station had the lowest snowpack depth and earliest melt date.

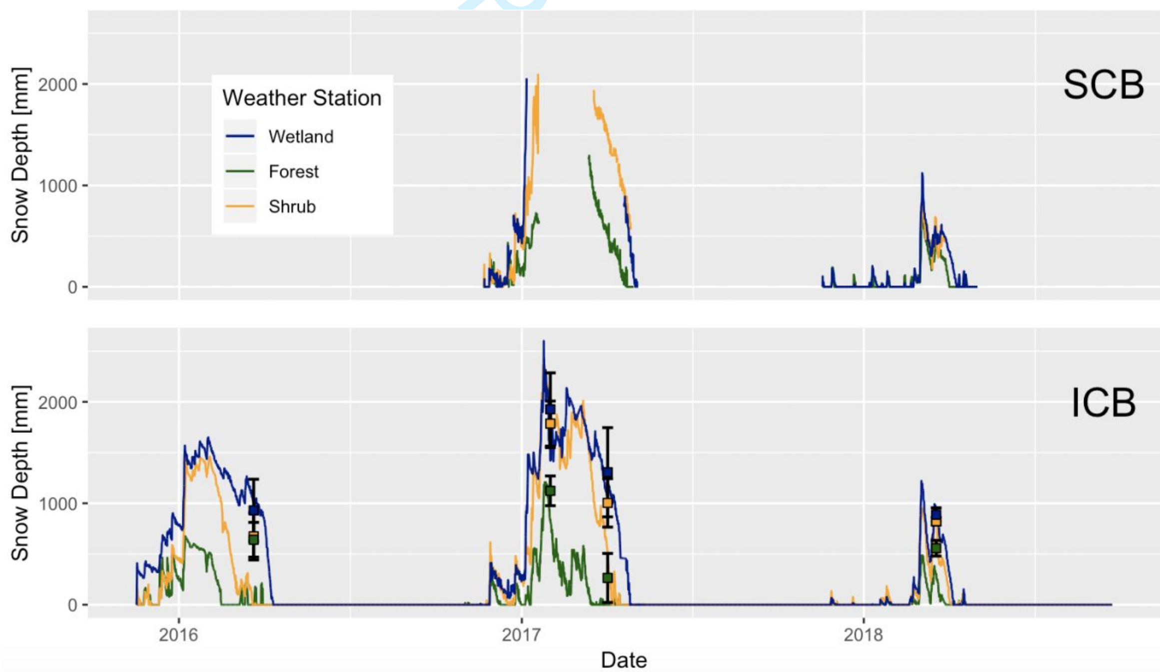

Figure B3: Snow depth (in mm) for Sugarloaf Creek Basin (top) and Illilouette Creek Basin (bottom) as measured from images taken four times each day at wetland, shrub, and forest weather station sites. Additionally, error bars (squares indicating mean, and bars indicating standard deviation) are shown for manually measured snow depths in ICB. In SCB, cameras were covered during peak snowpack for 2017-18 winter, resulting in missing data. Same winter shrub camera has stopped working before full snowmelt.

Appendix C: Details of landscape changes

Methods:

We used the FRAGSTATS package to calculate land cover metrics for ICB and SCB on vegetation maps created from images taken in 1973 and 2014 (SCB) and from images taken in 1969/70, 1987, 1997, 2005, and 2012 for ICB. For both watersheds, the first year of imagery (either 1973 or 1969/70) coincided with the end of a long period of fire suppression, and represents vegetation before the first fire in the managed wildfire era. The vegetation maps divided land cover into four vegetation classes: forest, shrub, sparse meadow, and dense meadow. For SCB, areas south of the southernmost extent of historical fires were removed from the landscape change analysis, since this area consisted mostly of isolated patches of vegetation surrounded by rock and caused misleading values (this was not necessary for ICB, which contained very little mapped vegetation in the rocky high-elevation areas). Isolated pixels surrounded by different vegetation types were removed from the maps before processing by merging them with the surrounding vegetation type, which minimized differences caused by small isolated patches that were likely due to classification error or would be difficult to capture the same way using two sets of imagery.

Landscape Metrics:

Diversity indices describe heterogeneity by measuring how patches of vegetation are distributed spatially across the landscape and capture fire-related landscape changes well (Romme 1982). We evaluated the following diversity metrics:

Shannon's Evenness Index (SHEI) is the *Shannon's Diversity Index* (calculated using information theory) divided by the maximum diversity given the number of cover types present

(McGarigal et al. 2012). An evenness index of 1 means that all vegetation types are equally represented in the landscape; higher evenness indicates greater landscape diversity.

Simpson's Evenness Index (SIEI) is similar, but is calculated using the probability that any two cells selected at random would be different patch types (McGarigal et al. 2012). Again, a value of 1 means all patch types cover an equal area, while a value near 0 means that one type dominated nearly all of the landscape. We include both evenness indices in order to verify that the exact method of calculating evenness does not affect our results.

Aggregation Index (AI) is a measure of how much each vegetation type is clumped into a few large groups (high aggregation) or spread into many small groups (low aggregation).

Patch properties within each class:

Patch properties describe local-scale heterogeneity and the size and shape of individual vegetation patches. For this study, we used metrics which have been shown to be consistent across many different landscapes (Cushman et al. 2008):

Largest patch percent area (LPI) gives the percent of the total vegetated area taken up by the largest contiguous vegetation patch within each vegetation class. This metric gives an idea of the maximum area dominated by a single type of overstory.

Fractal dimension (FRAC) measures how complex and plane-filling the shapes are by using the relationship between the area and perimeter of a patch. As the dimension approaches 2, perimeter is maximized for a given area of coverage, while for simple geometries such as squares or circles the dimension is 1 (McGarigal et al. 2012). For example: a vegetation class with a low fractal dimension whose largest patch covers a large area indicates a spatially homogeneous region. On the other hand, a high fractal dimension suggests an increase in the total length of boundaries between patches of different types, thus increasing local heterogeneity.

We also calculated the mean and standard deviation of the areas of all patches within each vegetation class. These measures help capture the changes in the distribution of patch sizes. All calculations were made on a rasterized vegetation map with a spatial resolution of 5 meters. This spatial resolution was chosen to match with calculations made on ICB vegetation (Boisramé et al. 2017b).

Results and Discussion:

Sugarloaf Creek Basin (SCB) showed a much smaller degree of landscape change than Illilouette Creek Basin (ICB). Diversity indices increased over time for both watersheds, but the change was negligible for SCB, showing that landscape diversity rose only very slightly in response to fire (Figure C1). The landscape-scale aggregation index increased slightly over time in SCB, in contrast to a decrease in ICB (Figure C2). This could be due to fires creating larger areas of sparse meadow that are more aggregated than pre-burn meadow areas (Figure C3b). The size of the largest vegetation patches did not vary appreciably in SCB between 1973 and 2014, with the exception of sparse meadows (Figure C3). The mean and standard deviation of patch sizes, however, showed similar trends to ICB (Figure C4). Most notably, conifer patches got smaller and less varied in size following 4 decades of fire (Figure C4). While fractal dimension increased for all vegetation types in ICB, it remained flat or decreased slightly in SCB (Figure C5). This may partially be due to fires creating a small number of new fairly homogeneous patches with simple geometries, but the small amount of change demonstrates that patch properties varied very little in response to fire in SCB.

Relative proportions of each vegetation type were similar between the two watersheds (Figure C6; note that these proportions do not account for exposed rock). Both watersheds also had similar Shannon's Evenness Index values in their pre-fire/post-suppression states (Figure C1). These similarities show that, despite differences discussed in the main text, the large-scale land cover types and distributions are comparable between these watersheds, making them useful to use as two case studies demonstrating how fire affects two similar landscapes in areas with slightly different climatology and geology.

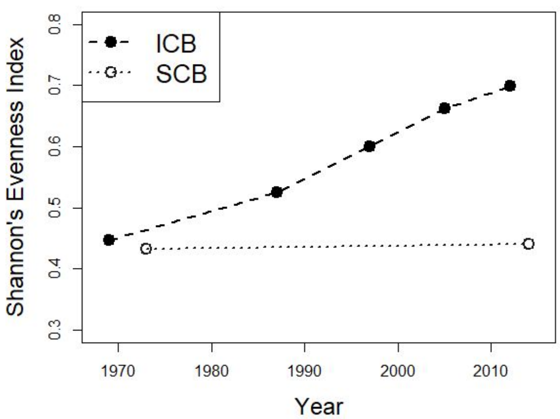

Figure C1. Shannon's Evenness Index calculated for both ICB and SCB for each year that we created vegetation maps from aerial imagery.

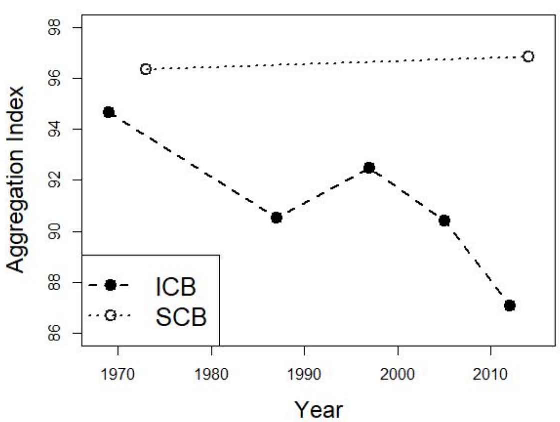

Figure C2. Aggregation Index calculated for both ICB and SCB for each year that we created vegetation maps from aerial imagery.

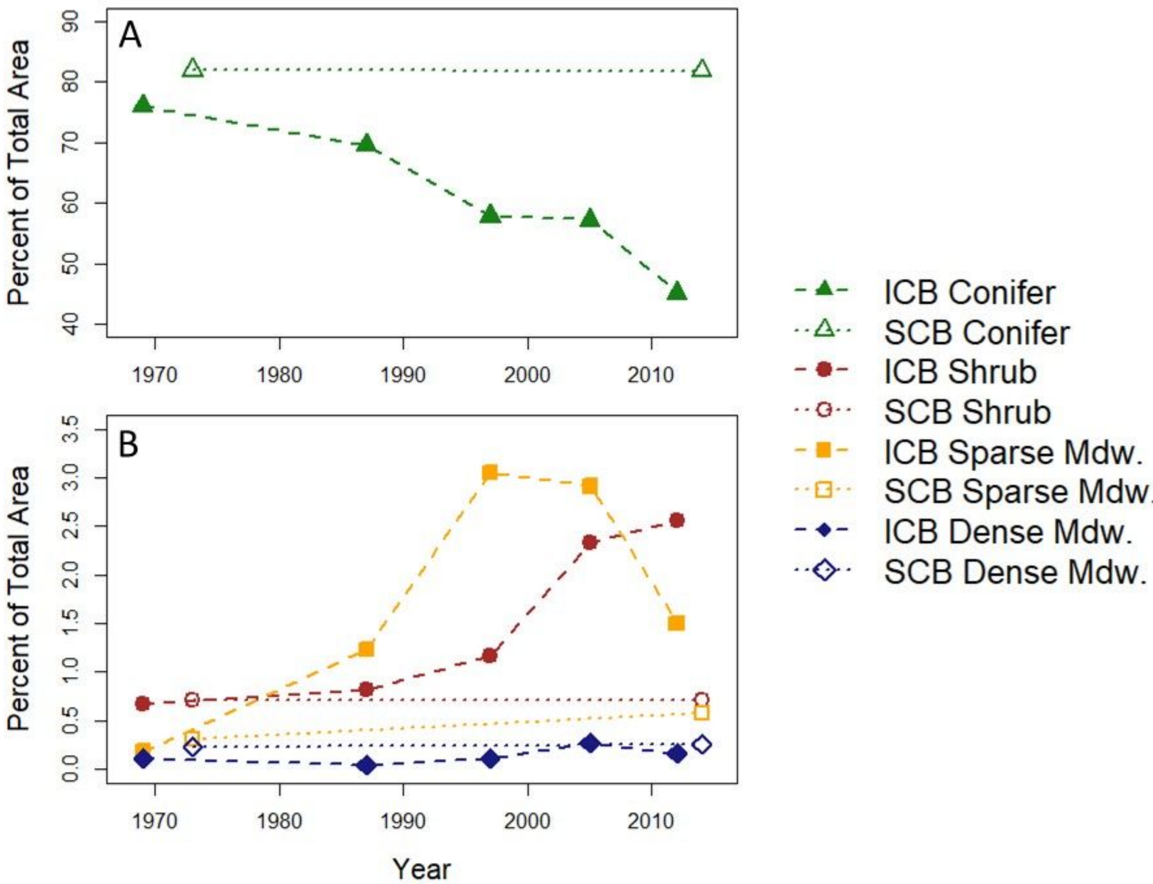

Figure C3. Largest patch index (LPI; the percent of the total area occupied by the largest contiguous patch of vegetation) for each vegetation class for both ICB and SCB. Conifer (A) is shown separately from the other vegetation classes (B) due to large differences in scale.

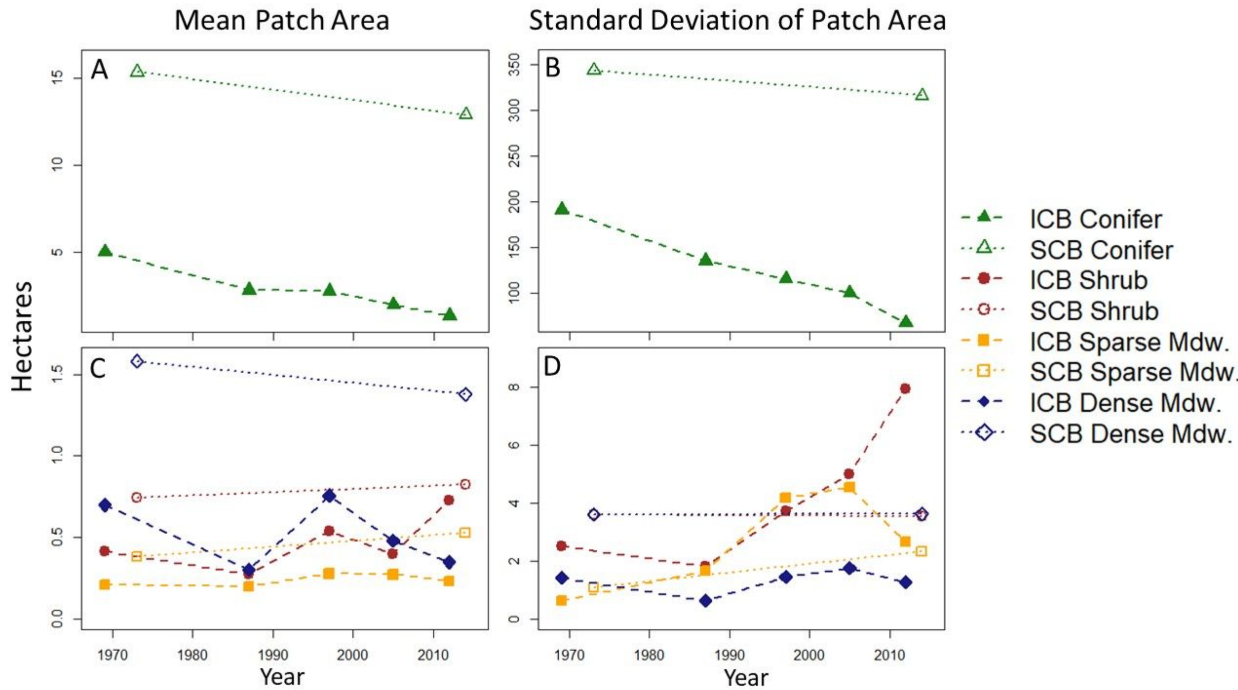

Figure C4. Mean (A,C) and standard deviation (B,D) of patch size for each vegetation class for both ICB (dashed lines) and SCB (dotted lines). Conifer is shown separately (A,B) from the other vegetation classes due to large differences in scale.

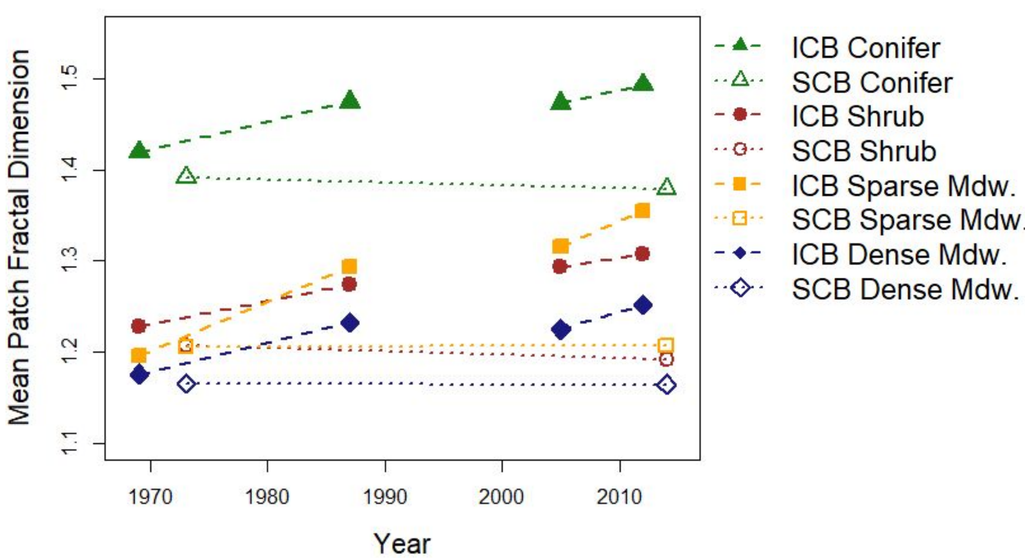

Figure C5. Mean area-weighted fractal dimension of patches for each vegetation class for both ICB and SCB. 1997 is omitted due to small differences in mapping protocol affecting patch fractal dimension.

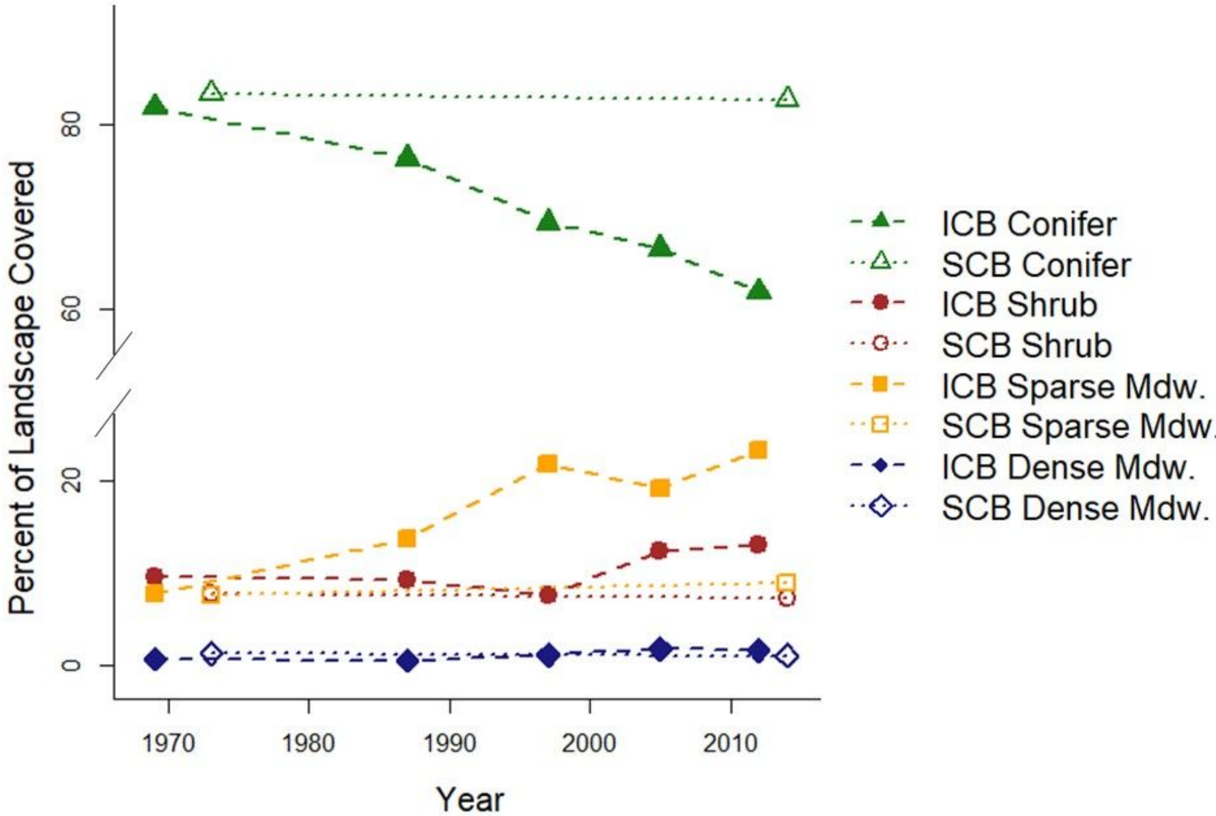

Figure C6. Percent of the total vegetated area covered by each vegetation class for both ICB and SCB.

Appendix D: Detailed soil moisture model results

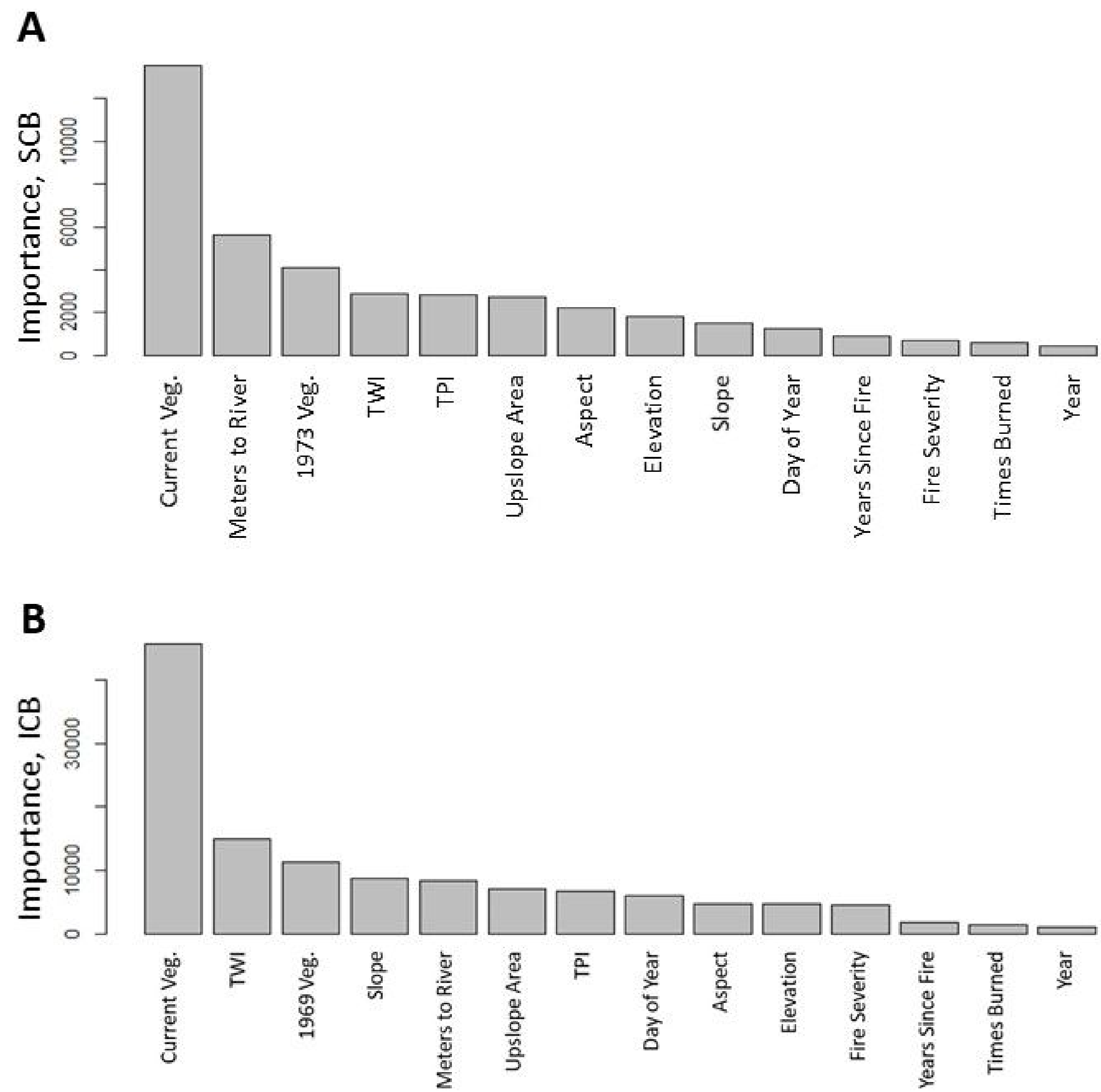

Figure D1: Relative importance of each variable in predicting plot-level soil moisture for Sugarloaf Creek Basin (A) and Illilouette Creek Basin (B). Variables include 2014 vegetation (Current Veg), Distance from nearest stream, 1973 vegetation, topographic wetness index at a 10m resolution (TWI), Upslope contributing area, topographic position index calculated at a scale of 300m (TPI), aspect, elevation, slope, maximum fire severity, days since January 1 for the measurement (Day of Year), years since fire, times burned, and year of the measurement.

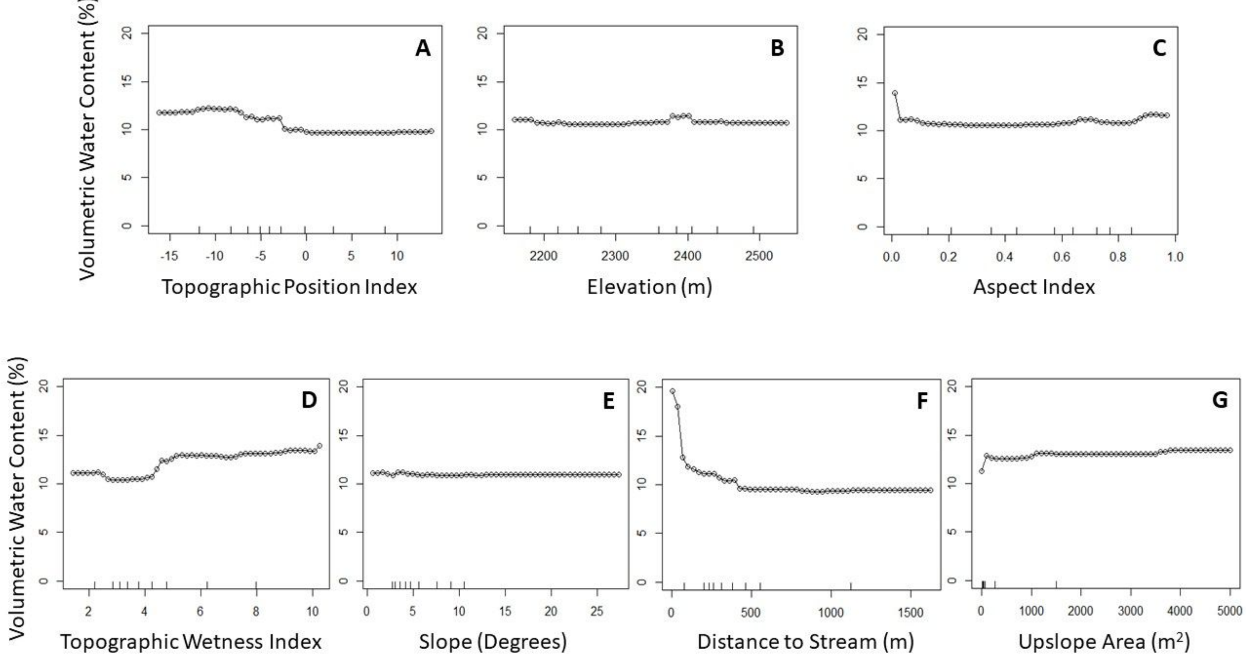

Figure D2: Partial plots showing how the mean soil moisture (across all other possible variable values) varies with each topographic variable.

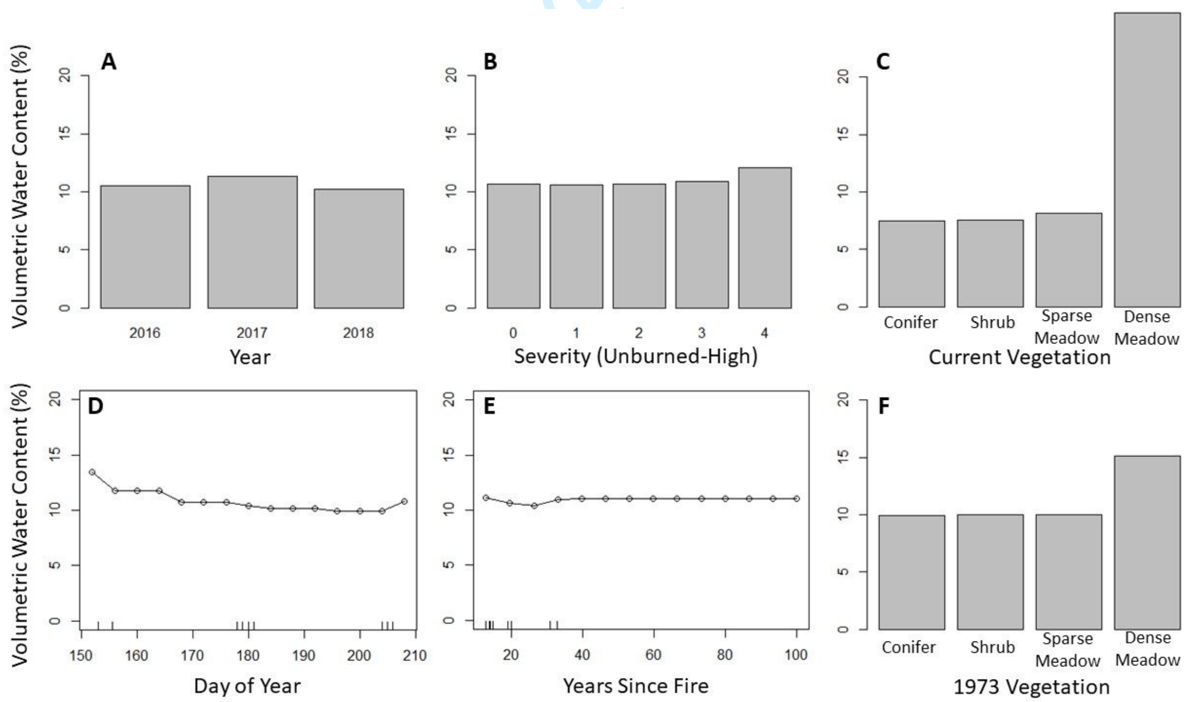

Figure D3: Partial plots showing how the mean soil moisture (across all other possible variable values) varies with each variable. Those variables treated as factors rather than numbers in the model are shown as bar plots. Number of fires varied moisture by less than 0.4%, and is not shown.

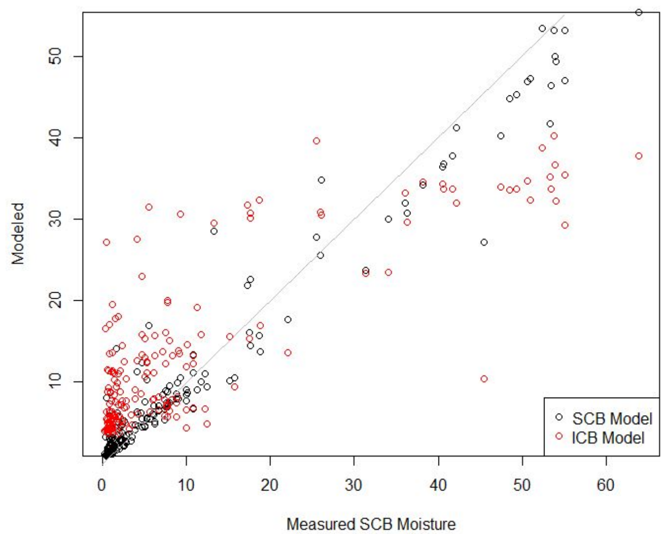

Figure D4. Modeled versus measured soil moisture in SCB (site means). Red points are calculated using a model trained on ICB data; black points are from a model trained on SCB data.

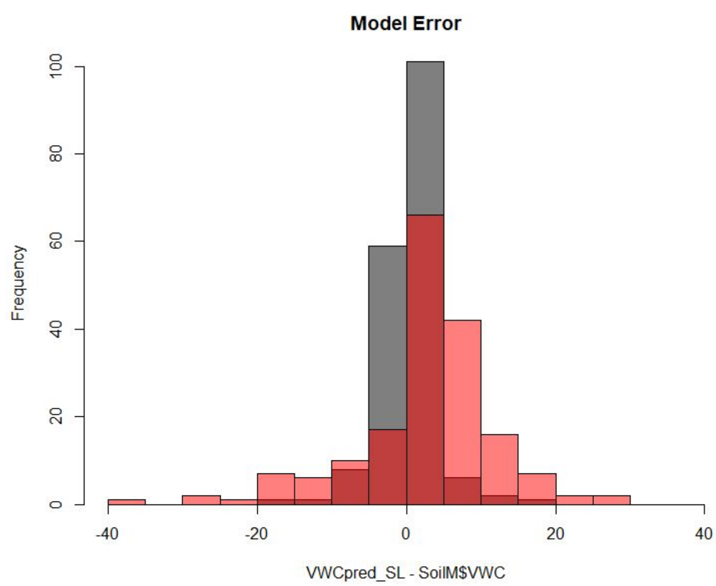

Figure D5. Errors in predicting SCB soil moisture using a model trained on SCB data (grey) and on ICB data (red).

Literature Cited

Boisramé, G. F. S., S. E. Thompson, M. Kelly, J. Cavalli, K. M. Wilkin, and S. L. Stephens. 2017b. Vegetation change during 40years of repeated managed wildfires in the Sierra Nevada, California. Forest Ecology and Management **402**:241-252.

Cushman, S. A., K. McGarigal, and M. C. Neel. 2008. Parsimony in landscape metrics: Strength, universality, and consistency. Ecological Indicators **8**:691-703.

Henn, B., A. J. Newman, B. Livneh, C. Daly, and J. D. Lundquist. 2018. An assessment of differences in gridded precipitation datasets in complex terrain. Journal of Hydrology **556**:1205-1219.

Little, R. J. A. 1988. Missing-data adjustments in large surveys. Journal of Business & Economic Statistics **6**:287-296.

McGarigal, K., S. A. Cushman, and E. J. Ene. 2012. FRAGSTATS v4: spatial pattern analysis program for categorical and continuous maps. Computer software program produced by the authors at the University of Massachusetts, Amherst. Available at the following web site: http://www.umass.edu/landeco/research/fragstats/fragstats.html.

Romme, W. H. 1982. Fire and landscape diversity in subalpine forests of Yellowstone National Park. Ecological Monographs **52**:199-221.